Environmental Microbiology

ENVIRONMENTAL MICROBIOLOGY

BRIEF REPORT OPEN ACCESS

Temporal and Spatial Dynamics of *Synechococcus* Clade II and Other Microbes in the Eutrophic Subtropical San Diego Bay

Katie J. Harding | Maitreyi Nagarkar | Maggie Wang | Kailey Ramsing | Niv Anidjar | Sarah Giddings | Bianca Brahamsha | Brian Palenik

Scripps Institution of Oceanography, University of California, San Diego, California, USA

Correspondence: Brian Palenik (bpalenik@ucsd.edu)

Received: 27 May 2024 | **Revised:** 2 September 2024 | **Accepted:** 25 October 2024

Funding: This work was supported by National Science Foundation, IOS-2029299, OCE-1637632.

Keywords: adaptation | bays | eutrophic | microbial evolution | microdiversity | *Synechococcus* | temperature

ABSTRACT

The diversity of the marine cyanobacterium *Synechococcus* can be broadly separated into clades, with clade II typically present in warm oligotrophic water, and clades I and IV found in cooler coastal water. We found amplicon sequence variants (ASVs) belonging to clade II in the nutrient-replete waters of San Diego Bay (SDB). Using the 16S rRNA gene, 18S rRNA gene and internal transcribed spacer region sequencing, we analysed multiple locations in SDB monthly for over a year, with additional samples dating back to 2015. *Synechococcus* community composition differed from the nearby coast into SDB in terms of dominant clade and ASVs. Specific clade II ASVs became relatively more abundant towards the back of the bay and showed seasonality, with higher relative abundance in the warm months. Select ASVs group phylogenetically and show similar seasonal and spatial distribution patterns, indicating these ASVs have adapted to SDB. Isolates matching clade II ASVs from SDB show pigment composition that is better adapted to the green light available in SDB, further supporting our findings. Other microbial taxa also show SDB enrichment, providing evidence that SDB is a chemostat-like environment where circulation, temperature, light and other environmental conditions create a zone for microbial evolution and diversification.

1 | Introduction

Marine picophytoplankton are important contributors to global primary productivity and are widespread throughout the world's oceans. The smallest of the marine picophytoplankton are the picocyanobacteria *Synechococcus* and *Prochlorococcus*, which can both be enumerated and distinguished by microscopy and flow cytometry (Chisholm et al. 1988; Collier and Palenik 2003). *Synechococcus* and *Prochlorococcus* are closely related to each other but are each comprised of distinct clusters of phylogenetically related strains with unique physiological characteristics contributing to their varied distributions globally (Rocap et al. 2002; Zwirglmaier et al. 2008). *Synechococcus* has a broader distribution including higher latitudes and nutrient-rich coastal regions, in addition to the open ocean (Flombaum et al. 2013).

The diversity of marine and estuarine *Synechococcus* has been organised into 3 subclusters, 5.1, 5.2 and 5.3, based on the 16S rRNA gene (Dufresne et al. 2008; Rocap et al. 2002; Scanlan et al. 2009). Subcluster 5.1 is the main marine subcluster and has been found to have the broadest distribution and the most genetic diversity. Subcluster 5.2 is typically present in estuaries and temperate coastal waters (Chen et al. 2006; Huang et al. 2012). Subcluster 5.3 inhabits similar environments as subcluster 5.1 clades II and III (Sohm et al. 2016), occurring

in specific marine transition zones with intermediate iron values but limiting phosphorus values (Ahlgren and Rocap 2012; Farrant et al. 2016), freshwater lakes in temperate climates (Doré et al. 2022) and is seasonally present in the Sargasso Sea (Ahlgren and Rocap 2012). Isolates of the subclusters have revealed that the global distribution of *Synechococcus* is made possible through a variety of adaptions, such as modes of nutrient uptake (Moore et al. 2002, 2005), motility (Toledo, Palenik, and Brahamsha 1999), chemical tolerance (Stuart et al. 2009) and light harvesting capability (Palenik 2001; Six et al. 2007). Light harvesting in *Synechococcus* is controlled largely by the phycobilisome, a protein complex composed of multiple proteins and attached pigments. The absorption spectrum of the cell is greatly affected by the ratios of these different proteins and pigments, and *Synechococcus* can acclimate (short term) and evolve (long term) in response to different regimes of light intensity and light colour in their environment (Alberte et al. 1984; Everroad and Wood 2012; Ong, Glazer, and Waterbury 1984; Palenik 2001; Six et al. 2007; Wood, Phinney, and Yentsch 1998).

Molecular analyses have revealed a finer scale of diversity within subclusters in the form of distinct phylogenetic groups known as clades (sometimes called ecotypes). Studies using functional genetic markers such as the RNA polymerase gene, *rpoC1* (Mühling et al. 2005; Palenik 1994; Toledo, Palenik, and Brahamsha 1999; Toledo and Palenik 1997), or the internal transcribed spacer region (ITS) between 16S and 23S rRNA genes (Ahlgren and Rocap 2012; Chen et al. 2006; Choi, Noh, and Lee 2014; Huang et al. 2012; Rocap et al. 2002) and other markers reveal approximately 20 clades in the marine subcluster of *Synechococcus* 5.1 (Mazard et al. 2012). The distribution of clades has been characterised in ocean basin scale studies (Bouman et al. 2006; Johnson et al. 2006; Malmstrom et al. 2010; Sohm et al. 2016; Zwirglmaier et al. 2008). Diversity within a clade, referred to as microdiversity, has also been discovered by comparative genomics studies and may be due to adaptations to differing temperature, light and nutrient regimes (Larkin and Martiny 2017), while toxin production or toxic metal resistance may be additional factors (Paz-Yepes, Brahamsha, and Palenik 2013; Stuart et al. 2009, 2013).

Marine *Synechococcus* clades have distributional patterns that show coherence within broadly defined ocean regions at global scales. These regions are generally defined by temperature, light quality and nutrient concentrations, which allows for a loose outline of where certain clades are expected to be the dominant type (Ahlgren and Rocap 2012; Doré et al. 2020). In marine subcluster 5.1, clades I through IV and CRD1 are the most commonly found clades. Clades I and IV typically cooccur and are considered cold water clades and are found in coastal waters in and above mid latitudes (Tai, Burton, and Palenik 2011; Tai and Palenik 2009; Zwirglmaier et al. 2008). While clades II and III are often found in nutrient-poor, warm water environments, clade II is found with high abundances throughout the subtropics, while clade III is more tropical with lower abundances and favours areas with lower phosphate and/or higher iron than clade II, which is found at mid-range Fe concentrations (Ahlgren, Belisle, and Lee 2020; Farrant et al. 2016; Sohm et al. 2016; Toledo and Palenik 2003; Zwirglmaier et al. 2008). CRD1 is also distributed in the tropics but specific to regions with low Fe (Sohm et al. 2016). Overall clade II is the most widespread clade with the largest available habitat in the warm, oligotrophic ocean (Farrant et al. 2016; Lee et al. 2019). As clade II is an open ocean inhabitant, it is optimised to use blue light with blue light-absorbing phycoerythrin proteins containing phycourobilin (PUB) chromophore pigments (Six et al. 2007). While temperature, light quality and nutrients often correlate with *Synechococcus* clade distribution at a global scale (Ahlgren and Rocap 2012; Doré et al. 2020), they do not fully account for temporal or spatial dynamics at a local scale (Ahlgren et al. 2019).

San Diego Bay (SBD) is a semi-enclosed basin in Southern California that is subject to anthropogenic influences. SDB serves a multitude of human and ecosystem services and is home to military operations, recreational boating and shipping. SDB is characterised as a low-inflow estuary as it receives intermittent freshwater inflow from the Sweetwater River, Otay River, Paleta Creek and Chollas Creek (Chadwick et al. 1996; Chadwick and Largier 1999a; Largier 2023; Largier, Hearn, and Chadwick 1996). As a result, it experiences seasonal shifts in subtidal circulation and exchange with the open ocean including periods where temperature dominates exchange and periods of hyperthermal and hypersaline conditions exist (Largier 2010). It also experiences complex longitudinal density gradients, which can lead to longitudinal zonation in water properties and estuarine circulation (Largier, Hollibaugh, and Smith 1997), which have been identified as defining distinct ecoregions (Sorensen, Swope, and Kirtay 2013).

SDB has hot spots of high concentrations of toxic materials such as copper (Cu) typical of an industrial port (Katz 1998; Neira et al. 2014; Blake et al. 2004). High Cu concentrations are of interest in the study of *Synechococcus* as studies have shown that they are particularly sensitive to it compared with other phytoplankton (de la Broise and Palenik 2007; Debelius et al. 2009; Le Jeune et al. 2006; Paytan et al. 2009; Debelius et al., 2010). Additionally, SDB has typically high chlorophyll 'green' waters. While the benthic fauna community composition in SDB has been investigated with respect to environmental monitoring and assessment (Hayman et al. 2020; Neira et al. 2014), few studies have investigated the microbial ecology of SDB (Klempay et al. 2021) or more specifically, the cyanobacterial ecology. Surprisingly, in a preliminary study, we found the SDB was often dominated by *Synechococcus* clade II, generally a blue light-optimised clade found in open ocean, oligotrophic waters.

In this study we compile a 1+ year monthly time series of *Synechococcus* sampling and sequencing data to investigate SDB *Synechococcus* community composition along a transect of SDB and compare it to a nearby coastal location at the Scripps Institution of Oceanography, Ellen Browning Memorial Pier (SIO). We sequenced the 16S rRNA gene and the *Synechococcus* 5.1 ITS region to investigate the unique *Synechococcus* populations in SDB. Furthermore, we analysed both 18S and 16S rRNA sequences corresponding to summer samples to provide a better picture of the overall microbial ecology of SDB. We also obtained isolates of *Synechococcus* from SDB to characterise their potential adaptations to SDB.

2 | Methods

2.1 | Sample Collection

Samples were collected from the Scripps Institution of Oceanography pier (SIO, 32°87′N, 117°26′W) and from SDB, monthly from July 2021 to September 2022 with additional samples in April, July and August of 2023. SIO samples were sampled the same day as SDB, except in August 2022 when SIO was sampled 4 days before and 4 days after the sampling of SDB. Additionally, four preliminary sample sets were collected from SDB in July 2015, March 2016, October 2016 and June 2019. SDB samples were collected in two ways. Full Bay transects (3 to 10 locations, Figure 2 blue icons) were collected by boat in July 2015, March 2016, October 2016, June 2019 and aboard the *R/V* Bob and Betty Beyster in August 2021, March 2022, May 2022, August 2022 and July 2023. Collections for all other months from July 2021 to September 2022 and April and August of 2023, were made from three shore locations within SDB (Figure 2, yellow icons) identified as MF (front bay), EM (mid bay), SS (back bay). Sediment samples were also collected in April 2023 from the 3 shore stations. We also included sequence data from the SIO pier from spring 2011, summer 2011, summer 2012 and summer 2016 sampling previously described in Nagarkar et al. (2021).

Samples were collected using a bucket to collect surface water and placed in polycarbonate 2–3 L bottles (acid-washed and rinsed 2× with seawater). Bottles samples were immediately brought to the laboratory (SIO samples) or kept cool in an ice chest (SDB Samples) until brought to the laboratory for processing later the same day. Samples for DNA extraction were filtered in duplicate (0.5 L) using 0.2 mm pore size Supor membranes (47 mm, Pall Corporation, Port Washington, NY, USA). Membrane filters were stored at −80°C until use. Sediment samples were collected using a handheld petite Ponar Grab. Sediment was collected in 50 mL Falcon tubes and kept on ice until frozen at −20°C until use. One millilitre of seawater was collected for flow cytometry analysis by fixing with 0.25% glutaraldehyde (Sigma-Aldrich, St, Louis, MO, USA) and incubating for 10 min at room temperature before storing at −80°C until use.

2.2 | Environmental Variables

The salinity and temperature of sampled surface water were collected on-site for SDB samples, by subsampling from the collection bucket as soon as it was retrieved. Salinity was determined by using a salinometer (accuracy/resolution: 0.05/0.5 psu), while temperature was recorded from digital (accuracy/resolution: 0.5/0.1°C) and alcohol (accuracy/resolution: 1/0.5°C) thermometers, for all months excluding August 2021. Temperature and salinity from the August 2021 boat transect were measured in situ with a vertically profiling SBE 25plus Sealogger CTD (salinity accuracy/resolution: $<0.04/<0.005$ psu, temperature accuracy/resolution: 0.001/0.003°C, Sea Bird Scientific, WA, USA), excluding stations 3, 8 and 10, which were measured as described for all other months. Temperature and salinity from SIO were taken from the Southern California Coastal Ocean Observing System (SCCOOS) data set (https://erddap.sccoos.org). Light spectra data were collected using a PRR-800 Profiling Reflectance Radiometer (Biospherical Instruments Inc. San Diego, CA, USA) by lowering the profiler to 1 m above the bottom 3 times. The EDZ channel values averaged over the 3 depth profiles were used for wavelength plotting. For all locations from July 2021 onward, 40 mL seawater subsamples were sent for analysis of dissolved inorganic nutrients (phosphate, silicate, nitrate plus nitrite and nitrite) to the Oceanographic Data Facility at SIO (La Jolla, CA, USA). Nutrients were measured using a Seal Analytical continuous-flow Autoanalyser 3. Protocols for measurements and analysis are described on the facility's website (https://scripps.ucsd.edu/ships/shipboard-technical-support/odf/documentation/nutrient-analysis). For chlorophyll concentrations, seawater was filtered on GF/F membranes (25 and 47 mm, Whatman) until the colour was visible (50–200 mL). Filters were folded and stored in tinfoil or cryovials and frozen at −80°C until sent for analysis at the Oceanographic Data Facility at SIO. Samples were measured on a Turner 10-005R fluorometer for Chlorophyll (mg/m^3) and Phaeophytin (mg/m^3) as described on their website (https://scripps.ucsd.edu/ships/shipboard-technical-support/odf/chemistry-services/chlorophyll). Rain (inches/week) and tide water levels information was collected from NOAA publicly available data.

2.3 | Flow Cytometry

Flow cytometry samples were thawed and run on a ZE5 Cell Analyser, Yeti (Bio-Rad, Hercules, CA, USA) at The Scripps Research Institute (La Jolla, CA, USA). Using an automated sampling mechanism, 40 samples were run at a time and 200 to 300 μL of each sample was run. Cell counts were analysed for *Synechococcus* and cryptophytes using FlowJo v10.8 Software (BD Life Sciences) by gating and counting cells with phycoerythrin and chlorophyll using the 488 nm laser with filter 670/30 (PerCP) for chlorophyll versus the 561 nm laser with filter 577/17 for phycoerythrin.

2.4 | DNA Extractions

DNA extractions were done using two methods. The first method used for samples from July 2015 to October 2021 was a phenol: chloroform extraction followed by further purification with the DNEasy Blood and Tissue Kit (Qiagen, Valencia, CA, USA) (34 samples) as described in Nagarkar et al. 2021. Samples from November 2021 to September 2022 and April, July and August of 2023 (85 samples) were extracted using a modified bead beating protocol as described below. The extraction methods were compared regarding DNA concentration and quality using a nanodrop spectrophotometer (ND-1000) and resulted in highly similar extraction efficiencies.

For the second extraction method, membranes were cut and split between 2 microcentrifuge tubes containing ~100 mL 212–300 μm acid-washed glass beads (Sigma, St. Louis, MO, USA) and 400 mL ATL buffer (Qiagen). For sediment DNA extractions, 0.5 g of sediment was placed directly in the microcentrifuge instead of membranes, but otherwise, the method stayed the same. Tubes were frozen in a dry ice and ethanol slurry and then quickly thawed at 65°C, repeated three times. Samples were then homogenised 1 × 1 min in a mini bead beater (Biospec Products, Bartlesville, OK, USA) before addition of

45 μL Proteinase K solution (20 mg/mL, Qiagen) and incubation at 55°C for 1.5 h. Four microlitre of RNase (10 mg/mL, Thermo Scientific) was added and the mixture was incubated at 65°C for 10 min with periodic mixing. Samples were then processed following the manufacturer's instructions for the DNEasy Blood and Tissue Kit (Qiagen). DNA concentration was measured by nanodrop and replicate extractions were pooled before DNA was stored at −80°C until sequencing.

2.5 | Primers and Sequencing

Sequencing at RTL—Extracted samples from July 2015 to October 2021 were sent for sequencing at the Research and Testing Laboratory (RTL) Genomics (Lubbock, TX, USA). Primers for the *Synechococcus*-specific ITS region MSd_ITSafusF (GGATCACCTCCTAACAGGGAG) and MSd_SYnafusR R (AGGTTAGGAGACTCGAACTC) (Choi, Noh, and Lee 2014) were used for amplification. The 16S rRNA gene was amplified using primers 515yF (GTGYCAGCMGCCGCGGTAA) and 806R (GGACTACNVGGGTWTCTAAT) targeting the V4 region from Parada, Needham, and Fuhrman (2016). The 18S rRNA gene was amplified using primers EUK1391F (GTACACACCGCCCGTC) and EUKBr (TGATCCTTCTGCAGGTTCACCTAC) targeting the V9 region (Amaral-Zettler et al. 2009; Stoeck et al. 2010). All regions were sequenced with paired-end 150 bp reads with an average of 10,000 sequencing reads using an Illumina MiSeq. Samples were processed according to the RTL company protocol. RTL genomics removed oligo-tags, demultiplexed and filtered the ITS sequences for length and quality.

Sequencing at Novogene—extracted samples from November 2021 to September 2022 were sent for sequencing at Novogene (Sacramento, CA, USA) using the ITS, 16S rRNA and 18S rRNA primers given above. Reads were paired-end 250 bp reads with a sequencing depth of 30,000 reads using Illumina HiSeq. Adaptors and primers were removed from raw reads before reads were filtered at Novogene for length and quality.

2.6 | Bioinformatics

For the ITS region, 16S rRNA and 18S rRNA sequencing primers were trimmed from complementary forward and reverse reads (RTL sequences) using CutAdapt (v3.4), (Martin 2011). All sequences (RTL and Novogene) were further verified for quality using FastQC (v0.11.9, Babraham Bioinformatics) and filtered based on a minimum Phred score of 33. Sequences from the two sequencing centers were denoised separately using the dada2 pipeline in QIIME 2 (QIIMEiime2-2021.8, Bolyen et al. 2019) where lengths were trimmed based on the sequence quality of the sample. Representative amplicon sequence variants (ASV) were counted across all samples and rarefied in QIIME 2 to the samples with the lowest number of reads (ITS:3537, 16S:5481, 18S:2938) to reduce bias caused by the different sequencing depths. ASVs that occurred less than 10 times were removed from the dataset. ITS region representative sequences and count tables were merged after de-noising for further analysis at the ASV level.

ITS ASVs were blasted (version; 2.12.0+, Altschul et al. 1990) against a *Synechococcus* ASV ITS database (Nagarkar et al. 2021) to determine clade association and ASV name. ASVs that were the exact match to ASVs found in the database were named accordingly, while ASVs that did not match exactly were named with numbers larger than 236. ASVs that were not represented in the database were searched against the Cyanorak database with blastn (v2.1) (http://cyanorak.sb-roscoff.fr) to determine likely clade affiliation. Clade designations were further checked and adjusted based on phylogenetic trees constructed with reference ITS sequences from *Synechococcus* (Cyanorak). ASVs clustering with the publicly available sequence KORDI-52 were assigned to clade II as studies that used genomes and longer sequences resolved its clade II affiliation (Doré et al. 2020).

The taxonomic affiliation of the 16S rRNA ASVs was determined using a QIIME 2 feature classifier (Bokulich et al. 2018) based on GreenGenes (13_8) (Mcdonald et al. 2012) that was trained to the primer set used for this study. We used a taxonomic confidence threshold of 70% for 16S and removed sequences identified as chloroplasts and mitochondria. Additionally, 16S rRNA sequences identified as cyanobacterial were searched against the Cyanorak database with blastn (v2.1) and NCBI for higher taxonomic resolution. The taxonomic affiliation of the 18S rRNA ASVs was determined using a QIIME2 feature classifier (Bokulich et al. 2018) based on SILVA (release 138) 18S rRNA database (Yilmaz et al. 2014) trained to the primer set used for this study. Sequences identified as bacteria, archaea or unassigned were removed from the analysis. 18S rRNA sequences were grouped at the order level for visualisation purposes, but if order-level taxonomic assignments were not available then the next highest taxonomic assignment available was used and denoted as phylum (p) or class (c).

2.7 | Phylogenetic Trees

Phylogenetic analyses and trees were conducted using Geneious Prime version 2024.0.7 (geneious.com). ITS region sequences of the top 10 ASVs of each clade (if available) and the ITS region from representative isolates (Cyanorak) were aligned using MUSCLE followed by manual curation, and phylogenetic trees were built based on maximum likelihood PhyML (Guindon et al. 2010) using Jukes–Cantor substitution, 1000 bootstrap value and the tree optimised for topology and branch length. Improved visualisation of trees was done in iTOL (Letunic and Bork 2021). The heat maps corresponding to the phylogenetic trees represent the percent presence of each ASV at each location group. Sequences across all seasons, excluding the SIO bloom in 2016 which were grouped separately, were counted as present or absent in each bay region (top axis) and marked as the percent of the total samples in each region (SIO_bloom:6, SIO:23, front:26, mid:26, back:23). Text in the rightmost column indicates whether the ASV is more often present at the Scripps Pier (SIO) or SDB when obvious patterns are present.

2.8 | Bay Groupings

To consolidate data and analyse patterns, we grouped samples into the categorical variables: bay locations and seasons. The stations were grouped into their bay location category (front, mid, back) based on temperature and salinity, consistent with

prior studies that identify clear hydrographic regimes within the bay and important circulation and residence time responses (Largier, Hearn, and Chadwick 1996; Rodriguez 2019; Sorensen, Swope, and Kirtay 2013). Of note our designations are similar to Sorensen et al., however, they identify two separate mid-bay regions which we keep together as a transitional region as recent work has shown the locations of these regions vary significantly seasonally (Rodriguez 2019 and Anidjar et al., 2024). The front bay (S1, S2, MF) has a short residence time and mixes regularly with the ocean. The back bay (S9, S5, SS) has a long residence time (around 50 days, Largier, Hearn, and Chadwick 1996) and mixing with ocean waters can be very limited, especially in warm months. The remaining stations (S3, S4, S11, S6, S7, EM) were grouped as mid bay and had intermediate qualities between the front and the back bay. Similarly, the stations were grouped into two general seasons: cool (December to May: winter and spring) and warm (June to November: summer and fall). Warm months can create hypersaline conditions in SDB compared with the surrounding ocean, while cooler months usually have higher precipitation in the region which lowers the salinity of SDB.

2.9 | Statistics

All analyses were made in R Studio using R version 4.3.0 (R Core Team, 2023). Numerical environmental variables and relative abundances of clades or ASVs by sample were compiled, and samples with missing values were removed from the analysis. Data was then normalised by subtracting the mean and dividing by the standard deviation before matrices were calculated using Spearman correlation. The correlation matrix was used to calculate a principal component analysis (PCA) with princomp in R. Scree plots and the contribution of each variable (Cos2) was calculated using FactoMineR (1.34, Lê, Josse, and Husson 2008).

2.10 | Synechococcus Isolates

Enrichments were initiated from SDB water after it had been brought back to the laboratory in PC bottles and kept cool on ice. 1–2 mL of 1.2 μm filtered (1.2 μm pore size PC membrane in swinnex holder) SDB water was inoculated into 20 mL of sterile enriched seawater medium F/4 (Guillard 1975). The enrichments were incubated at 22°C in 25 μmol quanta $m^{-2} s^{-1}$ of cool white light with 12:12 h light:dark. Enrichments were pour-plated once growth was visible as described in Brahamsha (1996) and colonies were picked and regrown in liquid media (F/4). For studies of growth at various temperatures, cultures were acclimated to temperatures between 10°C and 31°C for 2 weeks. The acclimated cultures were then transferred to fresh media and placed back at the respective temperature before growth measurements began. Growth was measured as relative fluorescence on a fluorometer equipped with a phycoerythrin excitation and emission filter set. The growth rate at each temperature was calculated as the slope of exponential growth when plotted as natural log (relative fluorescence). The excitation spectra were measured on exponentially growing cultures using a FluoroMax-4 spectrofluorometer (Horiba, CA, USA) with excitation measured from 350 to 660 nm and emission at 680 nm. Both excitation and emission slit widths were 5 nm with an integration time of 0.1 s.

2.11 | Figures

Figures and analyses were all made in R Studio (v4.3.0, R Core Team, 2023), using ggplot2 (v3.4.2, Wickham, 2016), Ocean Data View (https://odv.awi.de) or Excel (Microsoft).

3 | Results

3.1 | Comparison of San Diego Bay and the SIO Pier

Parameter averages show that SDB differs from SIO, with warmer temperatures and higher nutrient concentrations over the course of our study (Table 1). There are also notable differences within SDB in environmental parameters (Figure 1), consistent with

TABLE 1 | Comparison of collected surface measurements including inorganic nutrients from San Diego Bay (SDB) and the SIO Pier. Standard deviation (± st. dev.) represents variation across all SDB measurements in both time and space.

	San Diego Bay (mean ± st. dev.)	SIO Pier (mean ± st. dev.)
Temperature (°C)	20.54 ± 3.82	18.13 ± 3.06
Salinity (psu)	28 to 35.5	33.3 to 33.6
Ammonium (μmol/L)	1.02 ± 1.18	0.12 ± 0.08
Nitrate (μmol/L)	0.7 ± 1.1	0.32 ± 0.46
Nitrite (μmol/L)	0.12 ± 0.07	0.04 ± 0.03
Phosphate (μmol/L)	0.89 ± 0.25	0.32 ± 0.19
Silicate (μmol/L)	11.19 ± 4.45	2.7 ± 2.01
Chlorophyll (mg/m^3)	2.77 ± 1.95	4.14 ± 8.20
Syn (cells/ml)	$2.3 \times 10^4 \pm 3.5 \times 10^4$	$5.1 \times 10^4 \pm 2.7 \times 10^4$
Number of samples	63	16

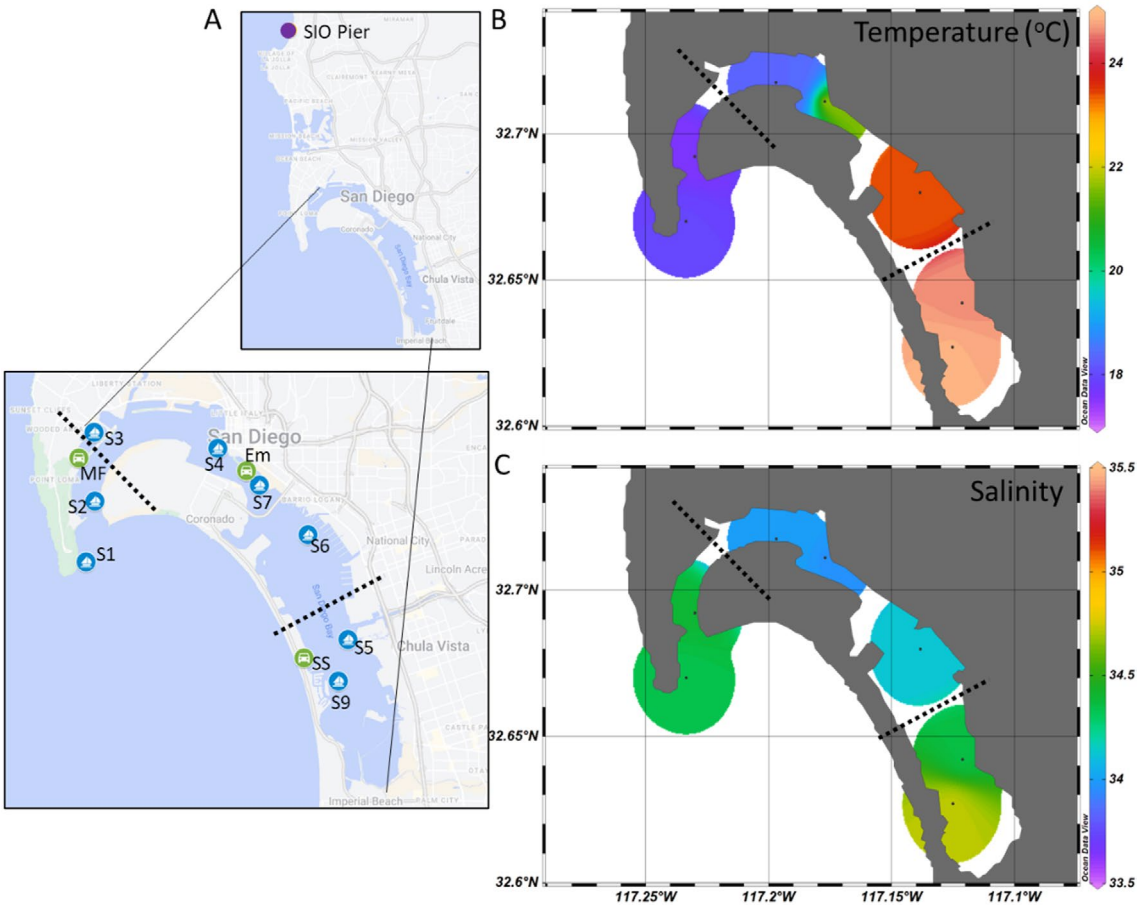

FIGURE 1 | Temperature and salinity of regions of the San Diego Bay. (A) Sampling locations at SIO Pier (purple dot) and SDB (inset). Dashed lines represent distinction between SDB regions; front bay (S1, S2, MF), mid bay (S3, S4, S7, S6, Em) and back bay (S5, S9, SS). For each boxed location, samples were collected from the shore (green dot), or by boat (blue dot). (A, B) Environmental variables from the SDB boat transect in August 2021 measured by SBE 25plus Sealogger CTD include (B) surface temperature and (C) surface salinity. For comparison SIO on the same sampling date salinity: 33.3 and temp: 21.1°C.

prior studies and recent observations (e.g., Largier, Hearn, and Chadwick 1996; Rodriguez 2019; Anidjar et al., 2024). The temperature is usually higher in the back bay and cooler in the front bay (Largier, Hearn, and Chadwick 1996; Rodriguez 2019), with exceptions only in winter months when temperature gradients are very weak and the back bay is sometimes colder (Figure 2. and Anidjar et al., 2024). Salinity varies in SDB based on location due to multiple points of intermittent freshwater input from watersheds and local sources. Figure 1 shows SDB in August 2021 with the highest salinity in the back bay and lowest salinity in the front bay. This hypersaline regime in the back bay persists for much of the year except when intermittent freshwater inputs occur (Figure 2, Rodriguez 2019 and Sorensen, Swope, and Kirtay 2013). The back bay and front bay end points of temperature and salinity create complex longitudinal density gradients with varying contributions of salinity and temperature (e.g., Largier, Hearn, and Chadwick 1996; Rodriguez 2019). Additionally, the light quality and attenuation in SDB changes from the front bay to the back bay (Figure S6). Surface waters in the front bay have a higher light attenuation overall compared to the back bay. Proportionally, the back bay also has more light in the yellow to red wavelengths (565–700 nm) than the front bay. Light quality with depth also shows a difference between the two stations.

Synechococcus abundances (cells ml^{-1}) are higher at SIO ($5.1\times10^4\pm2.7\times10^4$ cells ml^{-1}) year-round than in SDB samples ($2.3\times10^4\pm3.5\times10^4$ cells ml^{-1}), during 2021 to 2022 sampling. SIO often has blooms of *Synechococcus* as seen in November 2021, but even outside of bloom events, Synechococcus concentrations were higher at SIO compared to stations in the SDB at nearly all time points (Figure 2). SDB showed higher variability of *Synechococcus* abundances than SIO spanning three orders of magnitude with a range of 4.2×10^2 to 1.8×10^5 cells ml^{-1} while SIO remained within 2.7×10^4 to 1.3×10^5 cells ml^{-1}. A seasonal pattern for *Synechococcus* was not apparent for this data set. Using the boat-based spatial surveys of SDB in August 2021, March 2022 and August 2022, *Synechococcus* cell numbers (cells ml^{-1}) show a stark difference between SIO and front bay (S1 and S2) compared with the mid and back bay which have an order of magnitude fewer cells. However, in August 2022 we did not see clear differences in SDB regions due to the remarkably high *Synechococcus* cell numbers in the mid bay from a bloom at station 6.

Chlorophyll does not follow a gradient from SIO to back bay; instead, the highest chlorophyll concentrations (mg m^{-3}) are often in the front bay (7/14 months) or mid bay (5/14 months). One notably high chlorophyll concentration is present at the SIO in April 2022, due to a bloom of *Prorocentrum micans*, a non-toxic

dinoflagellate (https://habs.sccoos.org/scripps-pier). However, the chlorophyll concentration in SDB was much lower than SIO at the time of sampling, indicating the bloom was not in SDB.

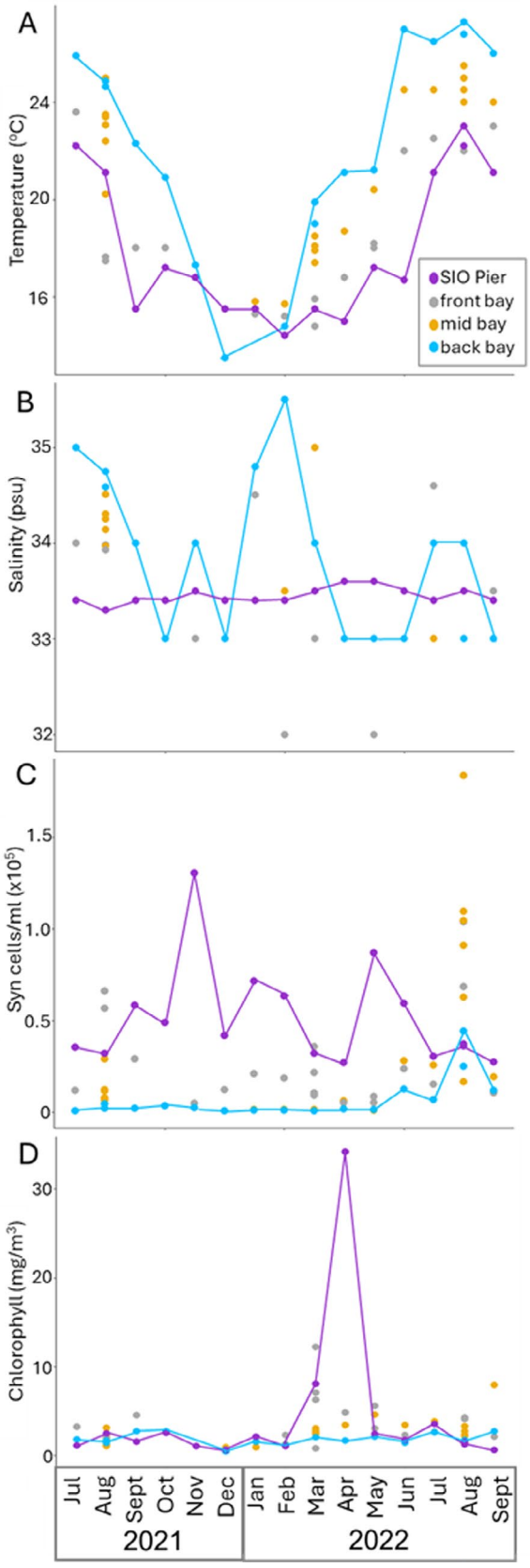

FIGURE 2 | Legend on next page.

A summary of all abiotic and biotic variables measured by the station can be found in Table S1. *Synechococcus* abundances at SIO and SDB, when analysed together, were not found to significantly correlate with any environmental variables measured in this study.

3.2 | rRNA Sequencing Reveals Gradients of Taxonomic Groups in SDB

The 18S rRNA sequence data reflects the gradient from the front bay to the back bay observed in the environmental data. The 18S rRNA sequence data from August 2021 (1073 ASVs) and August 2022 (1865 ASVs) boat transects through SDB (Figure 3) are grouped by taxonomy at the order level. The relative abundance of chlorophyte order mamiellales increased from the front bay (2021 avg. 3.1%, 2022 avg. 3.7%) to the back bay (2021 avg. 29.4%, 2022 avg. 28.8%), with lower relative sequence abundance at SIO (2021 avg. 1.5%, 2022 avg. 5.3%). Additionally, the cryptophyte order Cryptomonadales shows a smaller relative abundance but consistent presence in mid (2021:3.5%, 2022:4.4%) and back (2021:2.8%, 2022:4.3%) SDB as well. An additional transect was completed in July 2023 (Figure S3) and the pattern of higher relative abundances of Mamiellales in SDB was found then as well. The 18S rRNA data suggest that part of the higher relative abundances of Mamiellales is due to an *Ostreococcus* population (max. 32.8% in back bay 2021) with a unique ASV in SDB.

Using 16S rRNA data, the bacterial and archaeal community also shows changes in relative abundance along the gradients formed by SDB. The 16S rRNA sequences (Figure 3) show less fluctuation in taxonomic orders along the transect of SDB compared to the 18S rRNA data. However, there is a clear increase in the relative abundance of Rickettsiales in both August 2021 and 2022 from the front bay (2021 avg. 28.3%, 2022 avg. 8.2%) towards the back bay (2021 avg. 54.5%, 2022 avg. 20.4%) and a similar pattern was found in July 2023 (Figure S3). Higher resolution taxonomic assignment shows the majority of Rickettsiales are Pelagibacteraceae and it appears a specific *Pelagibacter* ASV (ASV454) becomes more abundant in SDB (2021 min. 21.7% front, max. 57.7% back, 2022 min. 6.4% front, max. 17.9% back) while ASVs 451 and 443 are more abundant at SIO (1.0%, 1.4% SIO respectively, 0% for both ASVs in back bay).

Synechococcus cell counts from flow cytometry are categorised into clades using relative percent abundance of the 16S rRNA sequences, assuming an equal number of 16S rRNA gene copies per

FIGURE 2 | Comparative seasonal dynamics of the SDB and SIO in surface water. (A–D) Monthly measurements from all locations from July 2021 to September 2022. The back bay (blue line) and SIO (purple line) data points are connected by lines to highlight the sampling location endpoints (i.e., oceanic in purple and furthest into the estuary in blue). Grey data points are data from the front bay and yellow data points are from the mid bay. (A) temperature (°C), (B) salinity, (C) *Synechococcus* cells ml^{-1} and (D) chlorophyll ($mg\,m^{-3}$). Samples were not taken from the mid bay in the Fall of 2021, and sample numbers differ by month according to boat sampling (10 stations) or shore sampling (4 stations).

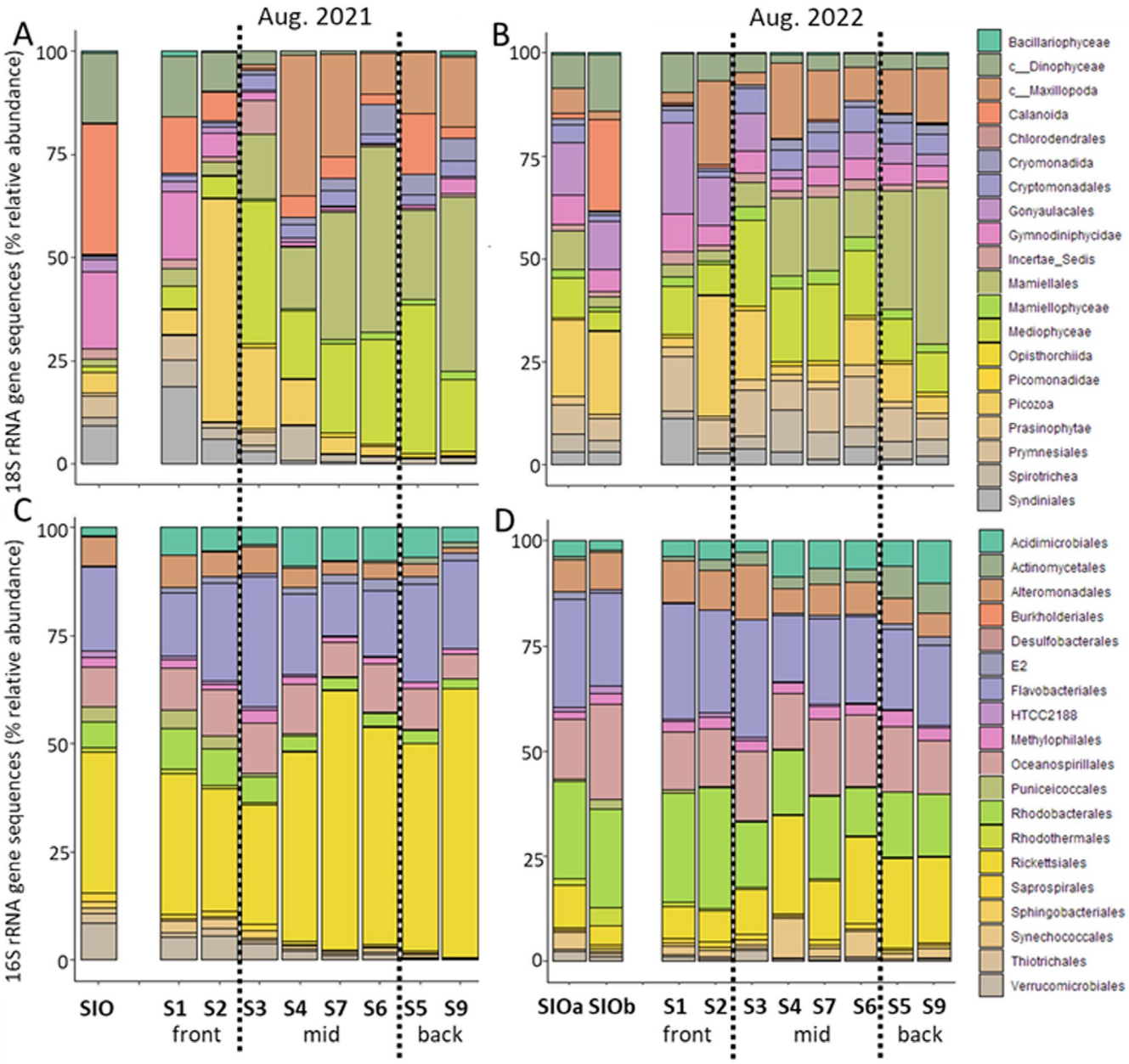

FIGURE 3 | Eukaryotic and Bacterial rRNA gene sequences for SDB transects. Relative abundance of top 20 18S rRNA sequences grouped by taxonomic order from August 2021 (A) and August 2022 (B). Taxonomic assignments starting with c__were only assigned at the class level. Relative abundance of top 20 16S rRNA sequences at the order level from August 2021 (C) and August 2022 (D). August 2022 SIO was sampled twice, corresponding to 4 days before (SIOa) and 4 days after (SIOb) the day the SDB was sampled. Dashed lines represent distinction between SDB regions; front bay (S1, S2), mid bay (S3, S4, S7, S6) and back bay (S5, S9).

cell, to get a qualitative representation of the relative abundance of the *Synechococcus* community (Figure 4). The 16S rRNA sequencing showed the presence of different *Synechococcus* subclusters and clades in SDB compared to SIOfrom summer samples from August 2021 and 2022 (Figure 4). August samples were chosen for spatial comparisons as *Synechococcus* abundances were previously seen to be highest in summer months in SDB (Table S1). Of the over 1 million reads of bacterial 16S rRNA gene reads, 4.5% were identified as cyanobacteria. ASVs that were identified as cyanobacteria included *Synechococcus* subcluster 5.1 (marine group) with 13 unique ASVs, subcluster 5.2 (estuary group) with 3 ASVs and a high light *Prochlorococcus* with 1 ASV. Making up 0.2% of the total cyanobacterial reads were the nitrogen-fixing organelle (Coale et al. 2024) UCYN-A (3 ASVs) and nitrogen-fixing cyanobacteria *Richelia* (1 ASV).

In SDB in August 2021, clades IV and I are the most abundant clades in the front bay, station 1 and station 2 (Figures S1 and S2). After S2, total *Synechococcus* numbers decrease towards the mid and back bay, and clade II, followed by clade IX, become the dominant clades in increasing proportions. During August 2022, although clades IV and I are dominant at SIO and present in the front bay, clade II is again the most abundant clade followed by subcluster 5.2 (rather than subcluster 5.1 clade IX).

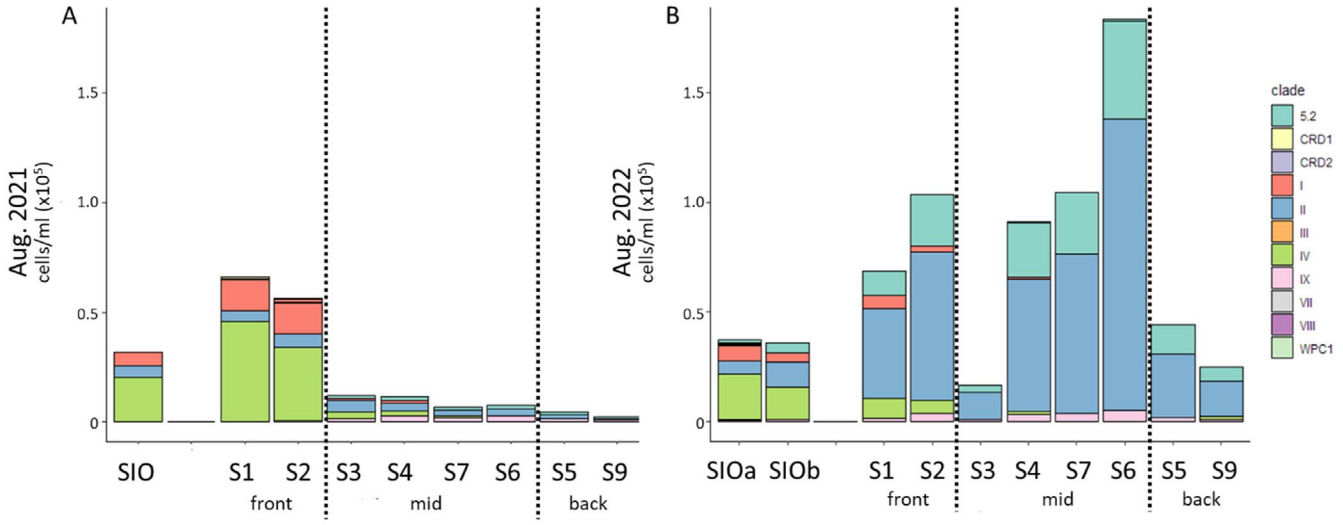

FIGURE 4 | *Synechococcus* community from 16S rRNA gene sequencing. *Synechococcus* cell counts are categorised into subcluster 5.2 or subcluster 5.1 clades using the relative percent abundance of each clade relative to the total *Synechococcus* 16S rRNA sequences, assuming an equal number of 16S rRNA gene copies per cell. August 2021 (A) and August 2022 (B) scaled to *Synechococcus* cells ml^{-1}. August 2022 shows the presence of subcluster 5.2, a typically estuarine subcluster. August 2022, SIO was sampled twice, corresponding to 4 days before (SIOa) and 4 days after (SIOb) the day the SDB was sampled. Dashed lines represent the distinction between SDB regions; front bay (S1, S2), mid bay (S3, S4, S7, S6) and back bay (S5, S9).

August 2022 had much higher *Synechococcus* cell abundances than August 2021.

Given the dominant presence of marine subcluster 5.1 including clade II in SDB, we chose to employ ITS primers as before (Nagarkar et al. 2021) to provide better sequence resolution of intra-clade diversity. However, subcluster 5.2 is not amplified by the ITS region primers as they are specific for subcluster 5.1. Subcluster 5.2 is likely not amplified due to several mismatches in the reverse primer region. Due to the possible presence of subcluster 5.2 cells in our monthly cell abundance time series, ITS sequence data was not plotted with respect to *Synechococcus* cell abundance data as an unknown proportion of the *Synechococcus* cells counted by flow cytometry may belong to subcluster 5.2. We do know that some fraction of subcluster 5.2 cells appear in flow cytometry counts as they were later identified in single-cell amplifications derived from flow cytometry sorting (Palenik, unpublished data).

3.3 | ITS Data Shows Spatial and Temporal *Synechococcus* Clade Dynamics in SDB

Using *Synechococcus* subcluster 5.1 ITS region sequencing spatial diversity was investigated with higher phylogenetic resolution along SDB transects (Figure 5). SIO is our oceanic endpoint and stations 1 and 2 in the front bay resemble the community composition of SIO at the clade and ASV level, which we would expect due to tidal mixing of the water. The mid bay is a transition zone between the front bay and the back bay where oceanic clades I and IV decrease and back bay members, clades II and IX, increase in relative abundance. The two bay seasons are shown in Figure 5, August 2021 and 2022 with warmer waters, and March 2022 with cooler waters. The warm months in SDB are dominated by clade II, followed by clade IX. The cooler month of March is dominated by clades IV and I, while clade II is nearly absent except for a small fraction in the back bay. Thus the ITS data mirror that of the 16S rRNA gene except for the lack of subcluster 5.2 in the ITS data.

We further investigated higher resolution temporal changes in the *Synechococcus* community of SDB with monthly samples over 14 months from each region of SDB compared to SIO (Figure 6A). Clade IV (green) was more relatively abundant throughout most of the year except for spring when clade I (red) became the dominant clade as has been seen previously found (Nagarkar et al. 2021; Tai, Burton, and Palenik 2011; Tai and Palenik 2009). We found that SDB back bay is dominated by clade II for most of the year except, as noted in spring when clade I becomes dominant. The back bay also has a high proportion of clade IX although it is less consistently present throughout the year.

We can observe correlations of clades and environmental variables when using a principal component analysis (PCA, Figure 6B). PCA-1 represents 47.6% of the variability observed and is best represented (Cos2) by clade IV and is in the opposite direction of the clade II vector. Clade II is also positively correlated with temperature, silicate and PO_4 (in order of most variability explained). PCA-2 represents an additional 25.7% of the variability for a total of 73.3% represented by the first two principal components. When looking at the Spearman correlation matrix (Figure S4) used to calculate the PCA, which includes all the numeric metadata and the sum of reads in each clade, some interesting relationships emerge. For instance, there are no correlations between *Synechococcus* abundances (cells ml^{-1}) or clade relative abundance and chlorophyll. This is likely because *Synechococcus* is not the dominant contributor to the chlorophyll concentration values and that other more abundant

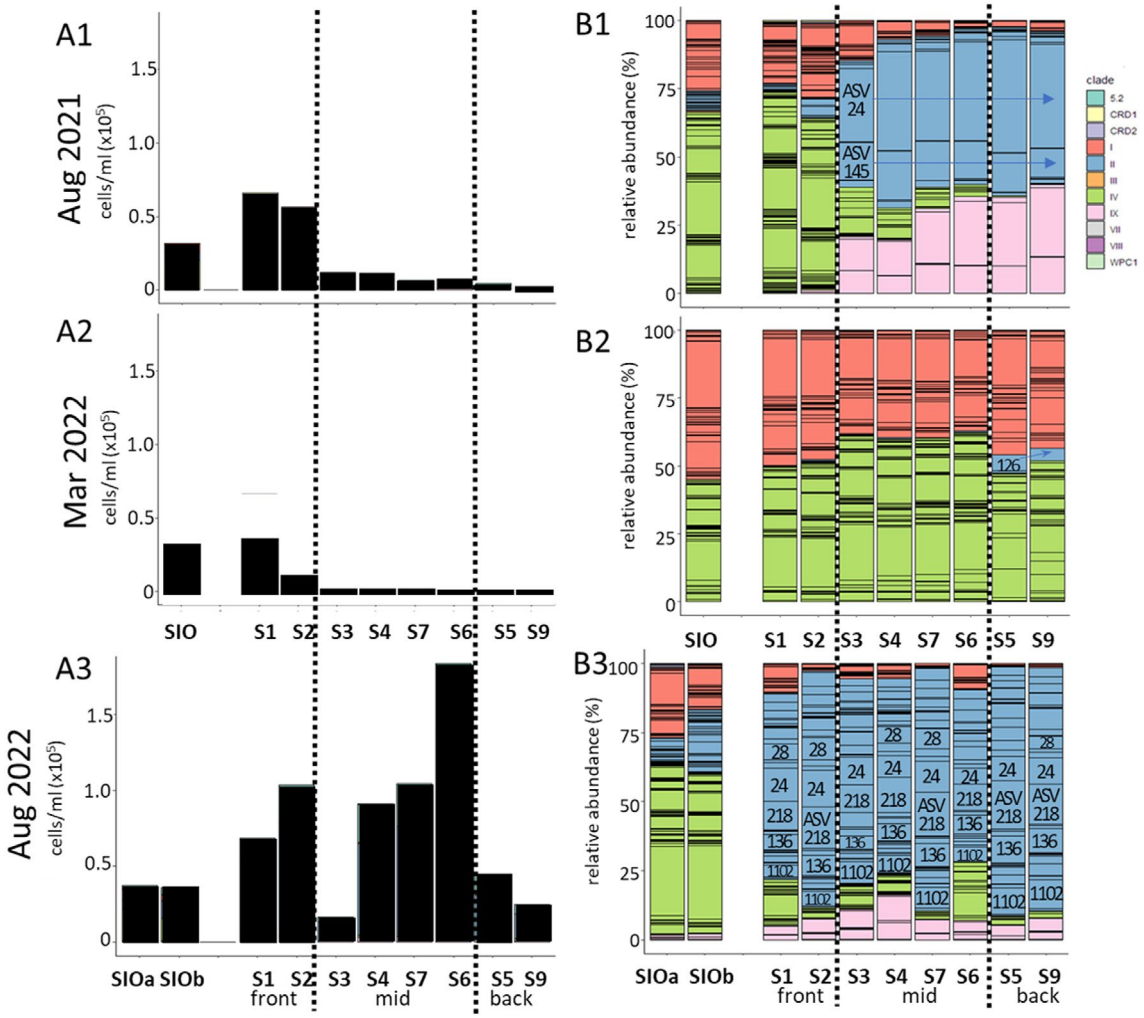

FIGURE 5 | Spatial distributions of *Synechococcus* abundances and subcluster 5.1 ITS diversity. *Synechococcus* abundances (A1–A3) and community composition (B1–B3) from August 2021, March 2022 and August 2022. (A) Synechococcus abundances (cells ml^{-1}) determined by flow cytometry organised by date (A1, A2, A3) and location (*x*-axis), the dotted vertical lines represent the bay location groupings; front, mid and back bay. (B) *Synechococcus* ASVs based on ITS region sequencing coloured according to clade affiliation organised by date (B1, B2, B3) and location (*x*-axis). Black horizontal lines within clade colours represent the relative proportion of ASVs. Clade II (blue) dominant ASV are labelled in the plot. ASV145 was a minor constituent in August 2022 ~ 10% of ASV218.

photosynthetic organisms are present as suggested by the 18S sequencing data.

3.4 | *Synechococcus* ITS Data Shows ASV/ Strain Dynamics

A Spearman correlation matrix (Figure S5) including the top 10 ASVs from each clade and available environmental variables shows that the ASVs follow similar patterns as the sum of the clade they belong to, which is expected. Clade IV ASVs correlate positively with clade I ASVs and most are negatively correlated with temperature, while clade II ASVs show a positive correlation with temperature and clade IX. A noticeable correlation between ASVs in clade IX and II is between the relatively most abundant clade IX ASV506g and clade II ASV24 (correlation coefficient 0.6). Both ASVs show a remarkably similar seasonal and spatial distribution. Lastly, clade II ASV126 stands apart in the correlation matrix as it does not follow a similar pattern to other ASVs in clade II or to clade II as a whole. ASV126 is the dominant clade II sequence type in SDB (78.6% of total sequences in back bay January 2022) and SIO (3.2% of total sequences SIO February 2022) during the cool season.

Synechococcus ITS ASV temporal and spatial analysis revealed fine scale dynamics that are not visible when looking at the clade as a whole or by using 16S rRNA gene ASVs. A phylogenetic tree comparing the top 10 ASVs for each of the 4 dominant clades shows variations in ASVs by location. We summarise this as the percent presence or absence of an ASV in a bay region including all dates sampled (Figure 7). As mentioned, clade IV is the most relatively abundant clade at SIO but within that clade there are at least two ASVs (ASV 2 and 4) that alternate dominance (Figure S6). The typically cold-water inhabiting clade I appears to have a back bay specialist, ASV210. Although not

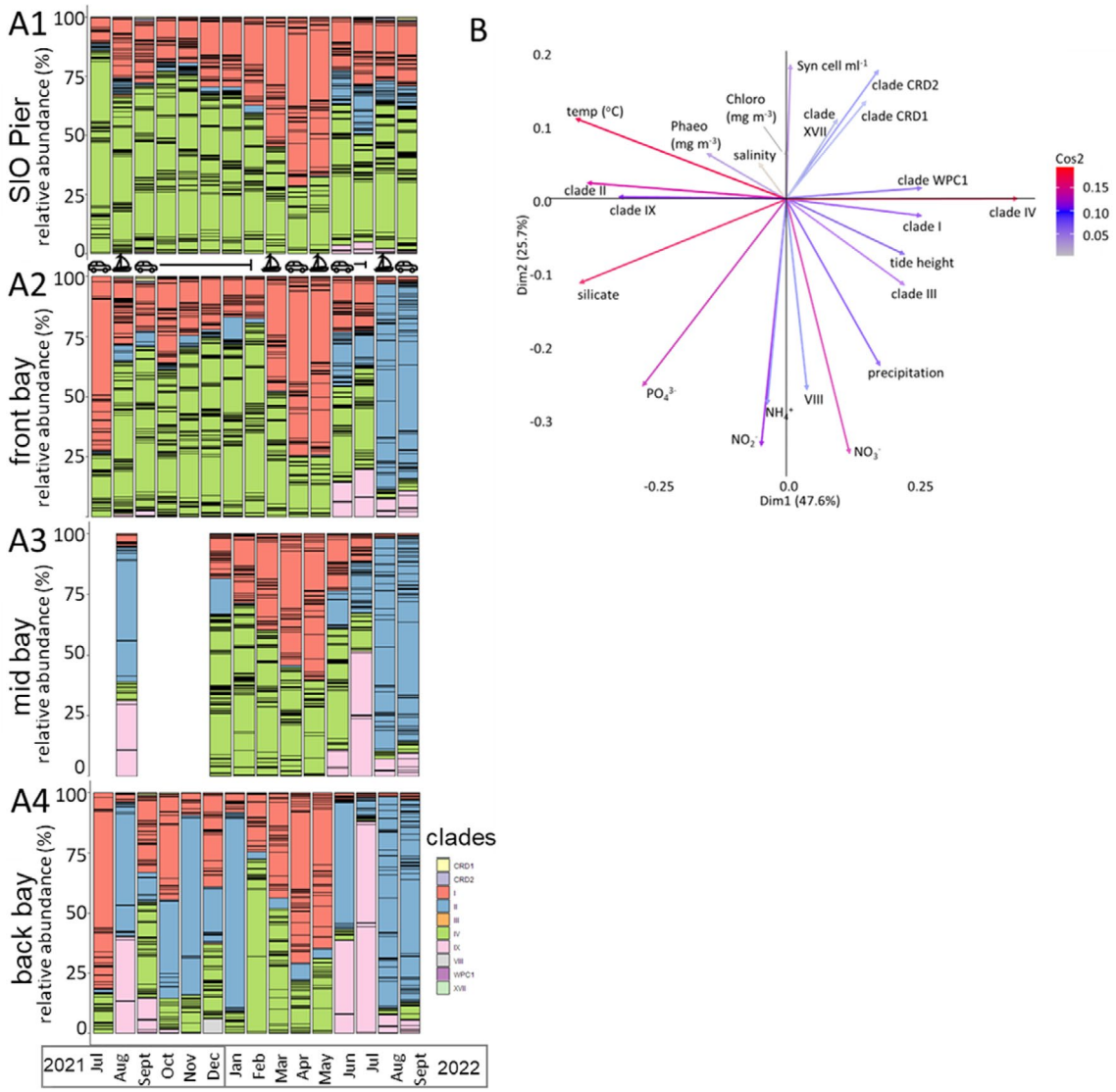

FIGURE 6 | Temporal changes in SIO and SDB based on *Synechococcus* 5.1 ITS diversity and community composition and ordination plots of *Synechococcus* ASVs from ITS region sequencing. Relative abundance of ITS sequences by geographic location (A1–A4) coloured by clade, black lines within clades represent unique ASVs and each bar represents a sample from each month. Between A1 and A2 the logos depict cars or sailboats to represent whether the SDB sample was collected from the shore (car) or during a boat transect (boat). Principal component analysis (B) of ITS ASV and environmental variable data plotted onto a 2-dimensional frame. The colour of vectors represents cos2, or the significance of that variable.

the dominant clade I ASV overall, the clade I ASV210 shows a higher percent presence in SDB (max. 22.2% back bay October 2021) than SIO (0% SIO October 2021). Clade I ASVs 291 (max. 7.7% back bay July 2021, 0% SIO) and 781 (4.8% back bay July 2021, 0% SIO) also show preference for SDB but with a lower overall occurrence. Clade IX has two clear SDB specific ASVs, ASV202 (max. 43.7% July 2022 back bay, SIO 1.6%) and 506 (max. 40.8% July 2022 back bay, SIO 2.8%). There is no evidence of a clade IX SIO ASV. Clade II is more relatively abundant in SDB and fitting with this pattern, several ASVs appear to be SDB specialists including ASV24 (max. 41.5% August 2021 back bay, SIO 0.8%), 145(max. 21.1% August 2021 back bay, SIO 0%), 120 (max. 4.3% Jun. 2022 back bay, SIO 0.9%), 25 (max. 4.2% Jul. 2022 mid bay, SIO 0.6%) and 28 (max. 50.1% Jun. 2022 back bay, SIO 2.1%). Additionally, ASV145 and 28 were present in sediment samples in the back bay in July of 2023, but absent in the water column at that time (Figure S7). Although many clade II ASVs are seemingly highly enriched in SDBASV119 (max. 1.5% October 2022 SIO excluding 2016 bloom, 17.5% August 2016 SIO bloom, 0% back bay) show a higher presence at SIO.

A detailed phylogenetic tree of all clade II ASVs (Figure S8) shows a high microdiversity within clade II with the majority of ASVs showing higher relative percentages in SDB. Clade II ASVs group into multiple phylogenetic clusters based on a maximum likelihood tree (phyML). One of the clusters in the phylogenetic tree includes ASVs 121 to 124 and additional higher numbered ASVs. These ASVs were prominent constituents of an anomalous clade II bloom at the SIO pier in 2016 and showed very low presence in the data set other than during the SIO bloom. However, although ASVs in that cluster made up a large portion of the SIO bloom community, ASV119 was the most relatively abundant ASV in the first 3 weeks of the bloom. ASV119 is an SIO-adapted clade II that stands somewhat alone phylogenetically but is

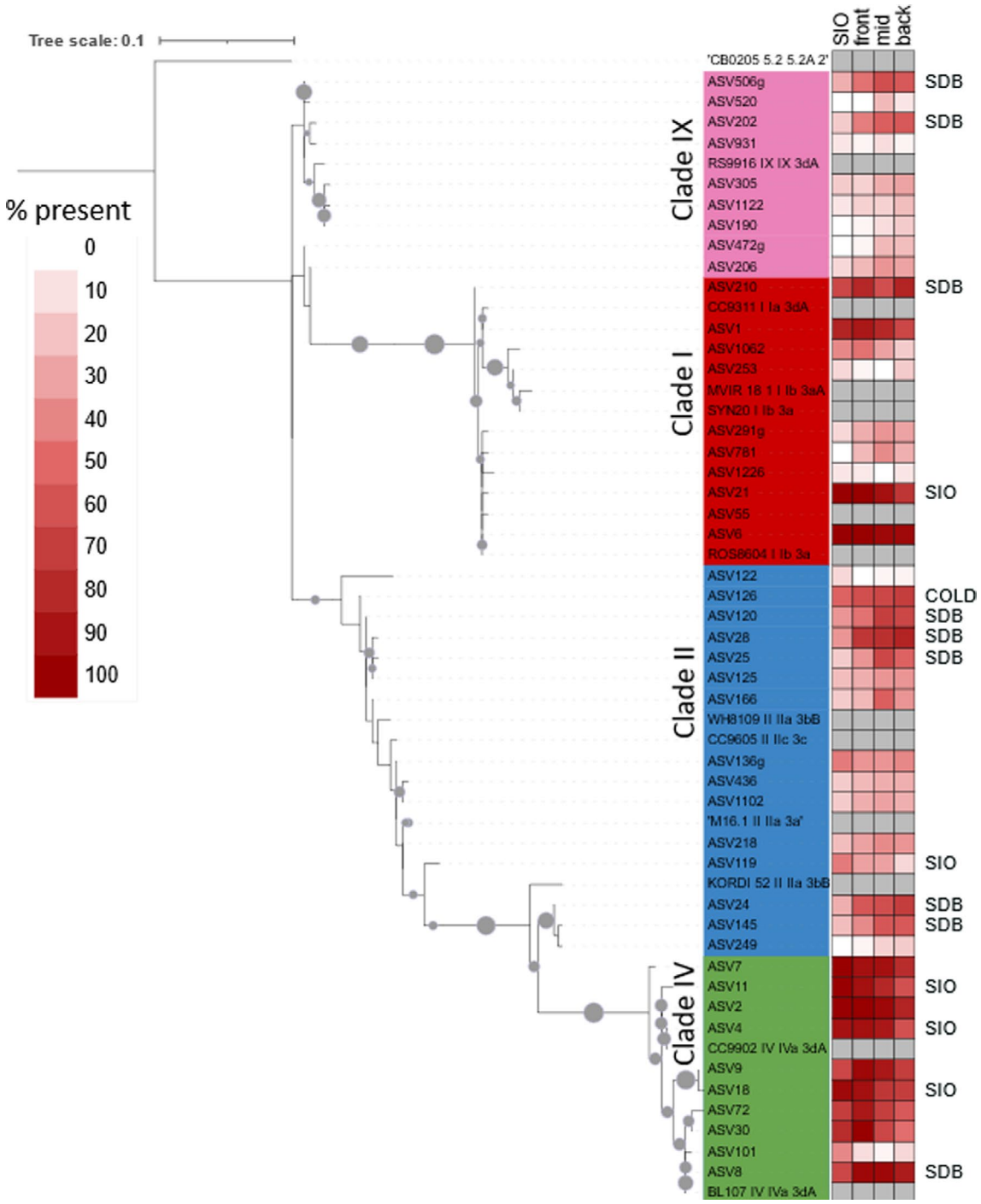

FIGURE 7 | Microdiversity within *Synechococcus* clades shows different presence and absence patterns at SIO and SDB. Shown is a maximum likelihood phylogenetic tree based on ITS nucleotide sequences of the top 10 most abundant ASVs from each of the 4 common clades. Grey circles represent bootstrap values over 30% based on 1000 iterations. Clade designations are shown in colour blocks: Clade I in red, Clade IV in green, Clade II in blues and Clade IX in pink. The heat map represents the percent presence of each ASV at each location group. Sequences across all seasons, excluding the SIO bloom in 2016, were counted as present or absent in each bay region (top axis) and marked as the percent of the total samples in each region (SIO;23, front;26, mid;26, back;23). Darker red corresponds to a higher occurrence of the ASV. Grey boxes represent isolates. Text in the rightmost column indicates whether the ASV is more often present at the Scripps Pier (SIO) or the San Diego Bay (SDB) when obvious patterns are present, or (COLD) in the case of the cold adapted ASV126, which is at SIO and SDB.

closest to the previously mentioned SIO bloom cluster. The later part of the bloom was dominated by ASV120, a SDB-adapted clade II (Figure S9), which is part of a broad cluster that includes SDB and SIO-specific ASVs as well as a few ASVs from the 2016 bloom. We had hoped that the ASV data would resolve the source of the large 2016 bloom, either from oligotrophic or from SDB waters, but this data is still ambiguous on this issue and it is possible the bloom taxa were seeded from different sources.

The last phylogenetic clade II cluster of note includes the reference strain KORDI-52 and clusters with ASV145 and ASV24, two of the most abundant SDB-specific ASVs in the dataset. Kordi-52 is considered a clade II strain based on genomic analysis (Doré et al. 2020) and longer 16S rRNA sequences. Thus, the diversity within clade II in SDB is phylogenetically widespread.

3.5 | *Synechococcus* Clade II Isolates

Although spatial and temporal differences in the relative abundances of ASVs can be identified, it is not possible to correlate these to the physiology of an organism harbouring a particular ASV sequence type without additional information. To begin to answer some of these questions, we enriched for and obtained *Synechococcus* isolates. Three non-axenic isolates of clade II *Synechococcus* were obtained from SDB: SDB1901, SDB1902 and SDB2102. Based on a comparison of the ITS region of the isolates and the SDB ITS ASVs, the isolates represent commonly occurring clade II ASVs in the SDB. All three isolates are within the top 10 most relatively abundant clade II ASVs. The ITS region of SDB1901 is 100% identical to clade II ASV145, a commonly occurring ASV in the bay during the warm season. The ITS region of SDB1902 is identical to ASV28, an often present and occasionally dominant ASV in the warm season. The ITS region of isolate SDB2102 is identical to ASV126, the cool season (SDB and SIO) dominant ASV.

We investigated the growth rate at various temperatures for the 3 isolates (Figure 8B) and compared that to the percent relative abundance of relevant clade II ASVs (Figure 8A) and found similar patterns based on temperature. SDB2102/ASV126 shows a maximum growth rate at 16°C but can sustain growth up to 31°C (the maximum temperature tested). This is consistent with the ITS sequence data that shows ASV126 is the most relatively abundant sequence type during the cool season, with the highest relative abundance at a temperature of 16°C. In contrast, SDB1902/ASV28 shows the highest growth rate at 23.5°C but is capable of high growth at temperatures from 20°C to 27°C. The ITS sequence data is consistent with these observations as the higher relative abundance of ASV28 occurs between 22°C and 29°C and it is often the dominant ASV in the warm season. SDB1901 has a lower growth rate than either of the other two isolates under these culture conditions but grows maximally at 24°C. SDB1901/ASV145 has a broader temperature range (high growth from 17°C and 24.5°C) than the other two isolates which show narrower peaks at the maximum growth temperature. The temperature range of SDB1901 is consistent with its ITS relative abundance as it has moderately high (up to 20%) relative abundances in the range of 19°C–25°C.

We also looked at the relative ASV abundance with respect to temperature for clades I, IV and IX (Figure S10). For clade I, the most common ASV, ASV6, had the highest relative abundance in the temperature range of 15°C to 21°C. Clade IV ASV2 has a broader temperature range from 15°C to 25°C although it occasionally showed higher relative abundance in the warmer range of 22°C to 25°C. Clade IX (ASV202 and 305) had the highest relative abundance from 23°C to 27°C.

In addition to temperature, the isolates exhibit differences in pigment composition, as seen in fluorescence excitation spectra (Figure 9). The isolates show excitation peaks at 495 and 545 nm for fluorescence at 680 nm which corresponds to the chromophores phycourobilin (PUB) and phycoerythrobilin (PEB), respectively. The ratios of PUB and PEB can vary in the phycoerythrin of different strains, and this can be used as

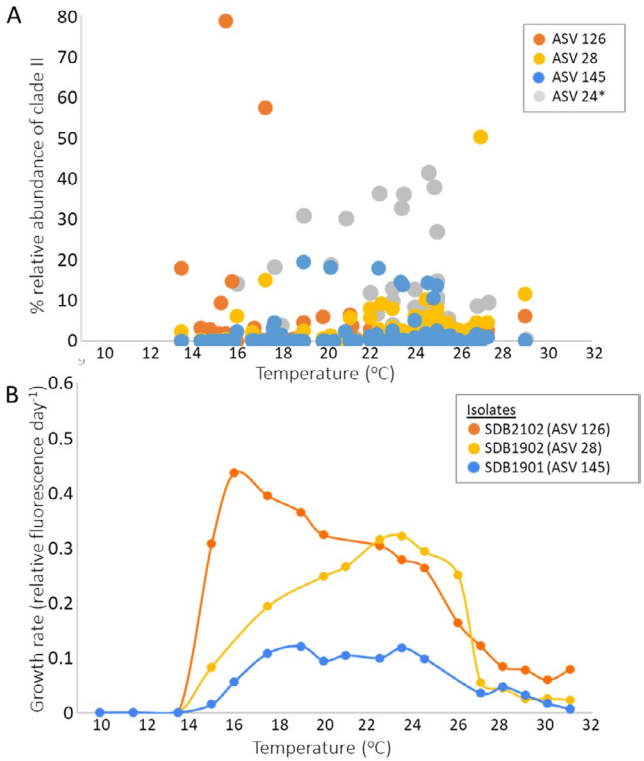

FIGURE 8 | SDB clade II isolate physiology. (A) The percent relative abundance of select ASVs within clade II based on ITS sequencing, ordered by sample temperature. Coloured circles highlight regions of higher relative abundance for each ASV. (B) Maximum growth rate (day^{-1}) by temperature for clade II isolates. Colours in A correspond to isolates (B) that are identical in the ITS region. *ASV24 (A) does not have a cultured representative in B but was included as it is relatively abundant ASV in the SDB at mid-range water temperatures.

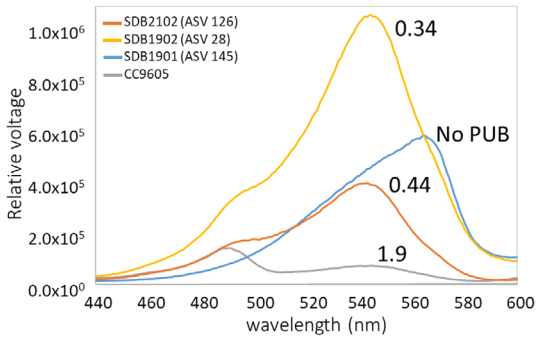

FIGURE 9 | Excitation spectra (440 to 600 nm) for clade II isolates for emission at 680 nm. An open ocean clade II isolate (CC9605) from previous studies was included for comparison. The spectra excitation peaks at 495 nm and 545 nm, which corresponds to the chromophores phycourobilin (PUB) and phycoerythrobilin (PEB), respectively. The PUB:PEB ratio for each isolate are noted on the figure.

an indication of the light wavelengths the organism is adapted to harvest. We have also included an open ocean clade II isolate CC9605 for comparison. CC9605 has both a PUB and PEB peak but has a higher ratio of PUB to PEB (1.9) making it a blue light specialist (Six et al. 2007), which is expected for an open ocean clade II strain. In marked contrast, SDB1902 lacks a PUB peak and therefore is likely to be green-light adapted. While SDB2102 and SDB1902 have peaks at PUB and PEB, their PUB:PEB ratios are 0.44 and 0.34, respectively. Strains with PUB:PEB ratios less than 0.6 are considered green-light specialists (Six et al. 2007).

4 | Discussion

Environmental data from SDB shows increasing silicate, phosphate, temperature and salinity towards the back bay. The back bay often experiences hyperthermal and hypersaline conditions (Figures 2 and 3) which is consistent with prior studies and suggestive of increasing residence times towards the back bay due to competing subtidal longitudinal circulation cells (Largier, Hollibaugh, and Smith 1997; Rodriguez 2019 and Anidjar et al., 2024) creating different niches for its microbial community. We grouped our sampling stations into front bay, mid bay and back bay sections based on these environmental variables and similar region delineation in prior work (e.g., Sorensen, Swope, and Kirtay 2013; Largier et al., 2010). The front bay is largely influenced by the surrounding coastal ocean waters mainly due to tidal pumping (Chadwick and Largier 1999a, 1999b). The back bay has the least oceanic influence and during warm summer months inverse estuarine circulation can form, isolating the back bay from the mid bay and increasing the residence time of the back bay water (Largier, Hollibaugh, and Smith 1997). The mid bay is a transition zone between the front bay and back bay, and, although it has a longer residence time than the front bay with less tidal influence, at least part of it is usually connected to the front bay by larger scale bay circulation (Largier, Hollibaugh, and Smith 1997). The longitudinal extent of the front bay oceanic/thermal regime and the back bay hypersaline, inverse regime vary seasonally and can extend into the mid bay regime to varying extents temporally. Light quality and attenuation also differs from the front bay to the back bay. The light quality available to organisms for photosynthesis is affected by the presence of other organisms, the concentration of coloured dissolved organic matter (CDOM) and suspended particulate matter (Mascarenhas and Keck 2018). Surface waters in the front bay have greater light attenuation compared to the back bay (Figure S2), which is in line with higher concentrations of chlorophyll in the front bay as more chlorophyll containing organisms would absorb the light and less would be available to be measured in the water column. Aside from the higher light values overall in the back bay, it has proportionally more light in the yellow to red wavelengths (600–700 nm).

To further understand the broader microbial communities present in SDB we analysed 16S and 18S rRNA gene sequences along two summer transects of SDB and other samples. The microbial community of SDB follows the hydrography. The front bay resembles SIO, our coastal reference point, in both eukaryotic and bacterial community composition while the back bay shows distinct differences in microbial community composition compared to SIO. Bay-specific populations of Eukaryotes (18S rRNA gene) and Bacteria (16S rRNA gene) have the highest relative abundance in the back bay (Figure 3). A few notable bay-specific populations of eukaryotes include diatoms, chlorophytes and cryptophytes. Diatoms of the order Mediophyceae are present throughout the back and mid bay, with lower relative abundances in the front bay. As a group, diatoms are well suited for SDB, which has higher silicate and other nutrient concentrations than the surrounding coast. Diatoms have been shown to have a broad range of tolerances for stressors such as heavy metals and pesticides, and low-light (Gottschalk and Kahlert 2012; Zhou et al. 2020). Cryptophytes of the order Cryptomonadales have an overall lower relative abundance compared to diatoms but are present throughout SDB, with lower relative abundances in the front bay and SIO. A recent study showed a few cryptophyte ASVs were more abundant in SDB than SIO (Rammel, Nagarkar, and Palenik 2024). Chlorophytes of the order Mamiellales were the most relatively abundant phylogenetic group in both August 2021 and 2022 in the back bay. The increase in the Mamiellales is due to increases in sequences closely related to *Ostreococcus tauri*, the lagoon associated *Ostreococcus* species (Chrétiennot-Dinet et al. 1995). Interestingly, the Mamiellales and *Synechococcus* clade II relative abundances show remarkable similarity in their relative increase towards the back bay and this may hint at a shared niche. However, although their niches may overlap, we observed a large bloom of *Synechococcus*, specifically clade II, in August 2022 but did not see the same increase in Mamiellales indicating different controlling factors for the two groups.

At the order level, gradients within the bacterial community composition determined by 16S rRNA sequencing are less dramatic than those in the eukaryotic community; however bacteria in the order Rickettsiales increase from the front bay towards the back bay, most of which belong to the family Pelagibacteraceae. When analysed at the 16S rRNA ASV level, the distinctions between SIO and SDB back bay were more dramatic, with specific ASVs in the above order becoming greatly enriched in the back bay. The 16S ASV data suggest that there are pairs of very closely related heterotrophic bacteria with different distribution patterns, eg SDB or SIO enrichment. This includes the family Pelagibacteraceae ASV454 (SDB) versus ASV451 and ASV443 (SIO) and the family Rhodobacteraceae ASV545 (SDB) versus ASV542 (SIO) as well as potential pairs in other families.

4.1 | *Synechococcus* Diversity in San Diego Bay

We conducted a 14-month time series and additional sampling that shows the presence of a group of typically oligotrophic *Synechococcus* (clade II) to be abundant in SDB. We used 16S rRNA gene and ITS region sequencing (Choi, Noh, and Shim 2013; Fuller et al. 2003; Nagarkar et al. 2021; Rocap et al. 2002) to characterise its dynamics. Overall, the spatial and temporal resolution of our sampling and especially the use of ITS sequences revealed *Synechococcus* clade II to be consistently present in the back bay and the most relatively abundant clade in 7 out of the 14 months sampled. At the ITS ASV level, there were more Clade II ASVs than ASVs for the other clades present. Different clade II ASVs were dominant over time. No seasonal pattern or spatial pattern was detected in the relative abundance of the different clade II ASVs. A previous study in the California

current system off Newport Beach found clade II microdiversity in the form of haplotypes based on the ropC gene showed significant seasonal variability (Larkin et al. 2020). Some recent evidence suggests ASV dominance changes may be due to short temporal scale factors such as runoff or viruses (Ahlgren et al. 2019).

Clade II is typically an open ocean *Synechococcus* clade, found widespread in the warm waters of the tropics and subtropics, in areas of low nutrients and midrange iron (Ahlgren, Belisle, and Lee 2020; Sohm et al. 2016). Although the SBD is warmer than the surrounding ocean it does not maintain a high temperature year-round like lower latitude locations. Additionally, SDB has higher concentrations of nutrients than the oligotrophic water where clade II is common (Ahlgren and Rocap 2012) and higher nutrient concentration than the surrounding Southern California coastal water where the dominant clades are I and IV (Larkin et al. 2020; Nagarkar et al. 2021; Tai and Palenik 2009). However, clade II is commonly found at low relative abundances in studies from the Southern California Bight, with a maximum estimated contribution of 20% of the total *Synechococcus* community (Larkin et al. 2020; Ahlgren et al. 2019; Lucas et al. 2011; Tai and Palenik 2009). One notable exception was one distinct bloom event in the summer of 2016 at SIO where clade II was the dominant clade in a *Synechococcus* bloom that reached 10^6 cells ml^{-1} (Nagarkar et al. 2021), surrounding this time frame a separate study along the Southern California coast noted an increase in clade II corresponding to the marine heat wave from 2015 to 1017 (Larkin et al. 2020). From these few studies it has been noted that the relative abundance of clade II is higher in later summer and fall (Ahlgren et al. 2019; Larkin et al. 2020; Lucas et al. 2011; Tai and Palenik 2009), which is in line with a positive temperature correlation seen in previous studies from the North West Atlantic (Ahlgren and Rocap 2012). In fact, clade II is found to consistently correlate with temperature in the open ocean (Xia et al. 2019) as well as more coastal locations (Larkin et al. 2020; Wang et al. 2022; Wang, Chen, et al. 2022). Clade II in SDB demonstrated a gradient of increasing relative abundance from SIO to the coastal ocean-influenced front bay and continuing to the back bay. The nearly year-round presence of clade II in SDB and high relative abundance of the clade during warm months show clade II is a resident of SDB that has adapted to the distinct environment of the bay.

In addition to temperature, clade II was also found to correlate with silicate and phosphate. Previous studies that investigated the presence of clade II with respect to nutrients have found conflicting correlations. For example, clade II was found to negatively correlate with phosphate and did not show a relationship with silicate (Doré et al. 2023; Xia et al. 2019). In other studies, clade II had a negative yet insignificant relationship with both (Wang et al. 2022; Wang, Chen, et al. 2022). Negative correlation with nutrients would be expected for the oligotrophic clade II (Ahlgren, Belisle, and Lee 2020). However, studies from coastal sites including Martha's Vineyard Coastal Observatory and a heavily anthropogenically influenced bay in the Bohai Sea in China, reveal clade II positively correlated with silicate (Hunter-Cevera et al. 2016; Wang et al. 2022) similar to our results from SDB. Including all the data from SDB and SIO, clade II positively correlated with temperature, silicate and phosphate. These contradicting correlations at the clade level from previous studies and the presence of distinct ASVs indicate that a finer taxonomic resolution may be required to understand these dynamics in different environments.

The *Synechococcus* community composition in SDB included other groups of note such as the little studied clade IX and the estuarine subcluster 5.2. Clade IX is noted in many studies as a minor constituent (Fuller et al. 2003; Laber et al. 2022; Wang et al. 2022), and while it is one of the dominant clades present in coastal Hong Kong (Xia et al. 2015), no general commonalities have been found linking its presence to a particular niche. Clade IX has also been found in the Gulf of Aqaba in the Red Sea (Fuller et al. 2003), tropical estuaries (Wang et al. 2022), the Gullmar Fjord in Swedish Skagerrak (Laber et al. 2022), and now SDB. In our study, Clade IX was a common occurrence in the back bay, and occasionally within midbay of SDB, where it was the most dominant clade type, as seen in July of 2022. Additionally, it showed positive correlation with clade II, a relationship that was also observed in a tropical estuary (Wang et al. 2022). As it was only seen on a few occurrences in the front bay and even less so at SIO, clade IX is another example of a back bay-adapted clade and potentially a future biomarker for extrusion of bay water out of the bay on short time scales.

Not as surprising is the presence of subcluster 5.2, a typically estuarine group and coastal water inhabitant (Ahlgren and Rocap 2012). SDB has some freshwater input from several creeks and rivers and more variable salinity than the surrounding coastal waters. However, SDB in summer to fall can become a hypersaline estuary due to long residence times, high evaporation rates and negligible freshwater input (Largier, Hollibaugh, and Smith 1997). Therefore, subcluster 5.2 likely has a broad salinity range as it is found in the hypersaline estuary of SDB (34 psu) as well as low salinity waters of the Chesapeake Bay, Luhuitou Peninsula and springtime Beaufort Sea (Wang et al. 2022). A semi-enclosed bay in the Western Yellow Sea showed subcluster 5.2 had a seasonal cycle with abundances increasing from winter to spring (Li et al. 2024). The presence of subcluster 5.2 in SDB and SIO was revealed by the analysis of the 16S rRNA data and would have been missed in the ITS region sequences data due to mismatches with the ITS primers designed to only amplify marine sublcluster 5.1. We have 16S rRNA data from August 2021, August 2022 (Figure 4), April 2023 (Figure S7) and July 2023, and subcluster 5.2 was present except in August 2021. It seems likely that the presence of 5.2 in SDB is common year-round as it occurs in both the warm and colder months.

The ITS ASV data provided a nuanced view of the *Synechococcus* microdiversity in the bay. Clade II had the most variability in dominant ASVs compared to the other the main clades present, I, IV and IX. In all these latter three clades, 2 to 3 dominant ASVs were present year-round and for the most part the dominant ASV stayed dominant throughout the year regardless of SDB or SIO location. Clade I ASV6 is the most relatively abundant clade I in our study year-round as well as in previous studies (Nagarkar et al. 2021). At the same time, both clade I and IV appear to have back bay specialist ASVs, ASV210 in clade I and ASV8 in clade IV. Although the clade IV ASV8 increases in the percent presence from the front bay to the back bay, the relative

abundance data suggest that it is surviving in SDB environment better than other clade IV ASVs, rather than specifically adapted to the environment. However, clade I ASV210 increases in both percent presence and relative abundance in SDB during the warmer months, indicating a preference for SDB. Clade I ASV210 shared 100% sequence identity with sequences recovered from the North Yellow Sea (Li et al. 2021).

Overall, while clade II ASVs are dominant in warm months in SDB, they vary over the six years analysed, with no clear pattern by season, location or determining environmental variable. This is in contrast to a nearby coastal studies that found two stable clade II microdiversity sequences that showed seasonal patterns (Larkin et al. 2020). Nevertheless, it is clear that many clade II ASVs are adapted to the environment of SDB. Relatively abundant clade II SDB specialists include ASV24, 145, 120, 25 and 28. To investigate whether these ASV are endemic to SDB or more widespread in similar hydrographic environments we used blastn to compare our sequences to the NCBI public database. We found sequences with 100% sequence identity over the whole sequence region match, ASV24 and 145, which were both recovered from the East China Sea (Choi, Noh, and Shim 2013). ASV120, ASV25 and ASV28 did not have a perfect match in the public database. The lack of sequence matches for many of our SDB specific clade II ASVs may indicate the these ASVs are specifically adapted to the SDB, while ASV24 ad 145 maybe be adapted to similar environments. However 100% similarity over the ITS regions does not necessarily mean identical genomes. A more detailed phylogenetic tree of clade II shows many more ASVs that are more abundant in SDB than at SIO. The multiple SDB-enriched ASVs as well as the apparent differences in community compositions between the SIO bloom and SIO compared to SDB suggest that clades II ASVs are a resident population in the bay and have adapted to the specific SDB environment, possibly multiple times.

The SDB-specific ASVs 24 and 145 phylogenetically cluster along with a high proportion of ASVs that are likely SDB specific, showing a higher percent abundance in SDB than SIO. ASV24 is the most relatively abundant ASV in summer August 2021 followed by ASV 145. ASV24 also makes up a sizable fraction of the clade II community composition in the summer of 2022, while ASV145 is present but with low relative abundances. This phylogenetic cluster also includes the reference sequence KORDI-52 and forms the most dissimilar cluster to other clade II ASVs. However, previous studies that used a longer region of the ITS cleanly resolved KORDI-52 into clade II (Cyanorak). Overall, this phylogenetic cluster is more present in SDB than the SIO pier and considering the consistent presence of ASV24 and 145 it is likely this cluster has acquired specific adaptations to be successful in SDB environment.

In April 2023, no clade II ASVs were detected in the water column, but ASVs 145, 28 and 1205 were found in sediment samples from the back bay. Although we have limited data, the occurrence of clade II in back bay sediments may be an indication of a sediment seed population that repopulates the water column once conditions are warming, a phenomenon that has been seen in cyst-forming dinoflagellates (Anderson and Wall 1978). This could explain the reoccurrence of clade II in SDB after their absence or near absence (excluding ASV126) in the early spring.

In our data, there is a clear difference in ASV presence at different temperatures (Figure S10) between the coastal clades I ASVs (15°C–18°C) and IV ASVs (15°C–23°C) and SDB clades II ASVs (22°C–27°C) and IX ASVs (23°C–27°C). The temperatures and ASV presence recorded in this study are in line with temperatures from a recent global metagenomic analysis that showed clade II was dominant where the average temperature was 27°C, clade I where the average temperature was 17°C, and clade IV where it was 19°C (Doré et al. 2022). Physiological investigations of our *Synechococcus* isolates belonging to dominant clade II ASVs from SDB suggest temperature is a strong determining factor in clade II ASV abundances. The isolates' temperature growth ranges and ITS relative abundance compared to environmental temperatures show very similar patterns regarding optimum temperature.

One particularly interesting finding was that ASV126 and its matching isolate SDB2002 show maximum ASV abundance and optimal growth at lower temperatures (16°C) compared with the other clade II isolates. ASV126 is the dominant clade II ASV in the cold months in SDB and SIO. The lower temperature growth range of SDB2002 is also different from that of other clade II isolates (M15-62 and M16.1) which were found to have maximum growth rates at 30°C and 34°C, respectively (Ferrieux et al. 2022; Pittera et al. 2014). Similarly, a previous study found different temperature preferences within clade I, indicating the microdiverity within clades supports a variety of temperature dependent physiological capabilities and therefore thermotypes within clades (Pittera et al. 2014). Although temperature can partially explain clade II ASV dynamics it does not explain them all. The presence of strains/ASVs with the ability to grow at lower temperatures than most clade II strains raises the question of how this may have occurred (the evolutionary mechanism) while also raising the question of how intraclade diversity may change in the future with a warming planet.

Marine *Synechococcus* express a number of chromophores suited to capture in situ light quality, and strains vary in the type and proportion of these pigments. PUB is a chromophore best adapted to the blue light wavelengths seen in oligotrophic waters (Wood, Phinney, and Yentsch 1998). *Synechococcus* clade designation does not predict pigment type (Carrigee et al. 2021; Six et al. 2007; Toledo, Palenik, and Brahamsha 1999) but most clade II isolates are type 3 (high PUB:PEB, although the ratio within pigment type 3 varies), as would be expected for a typically open ocean clade (Mahmoud et al. 2017; Sanfilippo et al. 2019; Six et al. 2007; Xia et al. 2017). The clade II isolates described here show adaptations to the light quality in SDB, the strongest example of strain adaptation to this niche. The isolates described in this study either lack PUB (SDB1901 (ASV145), pigment type 2) or have low PUB:PEB ratios (SDB2102 (ASV126) and SDB1902 (ASV28), pigment type 3). These are characteristic of green light-adapted organisms in contrast to the blue light-adapted strains such as the clade II open ocean strain CC9605. Our results are consistent with those of a recent study, in which pigment type 2 cells were found to be the dominant pigment type in the back bay of a semi-enclosed basin in the Western Yellow Sea, while blue light absorbing type 3 cells become the dominant type towards the outer bay (Li et al. 2024). Interestingly, AVS145 (ITS region match with isolate SDB1901) phylogenetically clusters with clade II isolate KORDI-52. KORDI-52 is blue

light adapted with a high PUB:PEB ratio and chromatic acclimation capabilities (CA4-B) (Carrigee et al. 2021) but SDB1901 lacks PUB altogether. Generally, pigment type 2 is uncommon for marine subcluster 5.1 (Grébert et al. 2018) but has also been found in a tropical clade II isolate isolated off the Saharan Coast, A15-44 (Carrigee et al. 2021; Grébert et al. 2018; Xia et al. 2017) like our SDB isolate SDB1901.

The presence of the typically open ocean clade II *Synechococcus* in SDB is intriguing. How did clade II find its way into SDB? What adaptations may it have acquired to survive in the anthropogenically influenced bay compared to the open ocean biome? Clade II is present in the coastal waters near SDB at SIO (Nagarkar et al. 2021; Tai and Palenik 2009) but it is rarely over 20% of the *Synechococcus* community (SIO annual avg. $5.1 \times 10^4 \pm 2.7 \times 10^4$ cells ml^{-1}). It has been speculated that clade II is present at SIO due to seasonal circulation, with highest relative abundances in late summer and fall (Tai and Palenik 2009). At that time, there is increased stratification that limits the cold, nutrient-rich water from upwelling while at the same time a northward flow begins in fall bringing oligotrophic warm water from the south (Ferris and Palenik 1998; Tai and Palenik 2009; Toledo and Palenik 2003). A similar hypothesis has been posed to explain the unexpected dominance of clade II in the Eastern Mediterranean Sea, where water from the Red Sea via the Suez Canal flows into the Mediterranean bringing in the clade II population (Doré et al. 2022). Although this makes logistical sense for the coastal waters it does not explain why clade II ASVs are abundant in SDB back bay because although there are typically warmer temperatures, there are also higher concentrations of nutrients as well as human induced harmful chemical concentrations including Cu (Katz 1998; Neira et al. 2014) and polycyclic aromatic hydrocarbons (Katz 1998; Hayman et al. 2020).

Novick and Szilard (1950) developed the now well-known concept and accompanying device called the chemostat. A steady inflow of media and outflow of cells creates an ecosystem with a population of cells at a steady state growth rate. However, they noted early on that a mutation in a cell could result in the cell outcompeting others and becoming dominant in the population. In their case it was an *E. coli* strain B/1/f that could grow faster on limiting tryptophan. Our data suggest that SDB is a chemostat-like environment where the temperature, light, nutrients, toxins and circulation regimes create an environment where selection acts on the resident microbial population, leading to new strains with better adaptations to the bay. The presence of strains all year, including a potential sediment reservoir, is important to this model. Future genomic and physiological studies of SDB clade II isolates could help determine the mechanisms of this adaptation. It is significant that these cells could also be exported to nearby waters and smaller bays, inoculating new strains into these smaller ecosystems.

Author Contributions

Katie J. Harding: writing – original draft, writing – review and editing, resources, data curation, investigation. **Maitreyi Nagarkar:** writing – review and editing, resources, data curation, investigation. **Maggie Wang:** writing – review and editing, resources, data curation, investigation. **Kailey Ramsing:** writing – review and editing, investigation. **Niv Anidjar:** writing – review and editing, data curation, investigation. **Sarah Giddings:** writing – review and editing, investigation. **Bianca Brahamsha:** writing – original draft, writing – review and editing, funding acquisition, investigation. **Brian Palenik:** writing – original draft, writing – review and editing, data curation, resources, funding acquisition, investigation.

Acknowledgements

We would like to thank Brett Pickering, Richard Walsh for captaining the R/V Bob and Betty Beyster. We are very thankful to Brian Seegers at the Scripps Research Institute for his valuable support with flow cytometry. We thank Angel Ruacho for help with initial samples to develop this work and Dr. Jackie Collier for early flow cytometry observations in SDB in the 1990s that suggested multiple *Synechococcus* populations. We are also grateful to Elliot Weiss and Greg Mitchell for use and deployment of the PRR 800, Phil Zerofski for use of the sediment grab, and Marina Frants for help with data archiving. This work was funded by the National Science Foundation (NSF Grant IOS- 2029299 to BP and BB). REU Funding for M. Wang was provided by NSF Grant: OCE-1637632.

Conflicts of Interest

The authors declare no conflicts of interest.

Data Availability Statement

All data are provided within the article and supplementary files, while sequences are openly available in NCBI GenBank under Bioproject PRJNA883423: https://www.ncbi.nlm.nih.gov/bioproject/PRJNA883423. ITS region sequence data are accessions numbers SAMN41478632 to SAMN41478741, 16S rRNA gene sequence data are accession numbers SAMN41479051 to SMN41479086 and 18S rRNA gene sequence data are accessions numbers SAMN41479268 to SAMN41479295. The ASV list for each amplified region can be found in the supplementary file ASV_list. Our supplementary data can now be found at: https://portal.edirepository.org/nis/mapbrowse?packageid=knb-lter-cce.323.1. or Datazoo at https://oceaninformatics.ucsd.edu/datazoo/catalogs/ccelter/datasets/323

References

Ahlgren, N. A., B. S. Belisle, and M. D. Lee. 2020. "Genomic Mosaicism Underlies the Adaptation of Marine *Synechococcus* Ecotypes to Distinct Oceanic Iron Niches." *Environmental Microbiology* 22, no. 5: 1801–1815. https://doi.org/10.1111/1462-2920.14893.

Ahlgren, N. A., J. N. Perelman, Y. C. Yeh, and J. A. Fuhrman. 2019. "Multi-Year Dynamics of Fine-Scale Marine Cyanobacterial Populations Are More Strongly Explained by Phage Interactions Than Abiotic, Bottom-Up Factors." *Environmental Microbiology* 21, no. 8: 2948–2963. https://doi.org/10.1111/1462-2920.14687.

Ahlgren, N. A., and G. Rocap. 2012. "Diversity and Distribution of Marine *Synechococcus:* Multiple Gene Phylogenies for Consensus Classification and Development of qPCR Assays for Sensitive Measurement of Clades in the Ocean." *Frontiers in Microbiology* 3, no. JUN. https://doi.org/10.3389/FMICB.2012.00213.

Alberte, R. S., A. M. Wood, T. A. Kursar, and R. R. L. Guillard. 1984. "Novel Phycoerythrins in Marine *Synechococcus* Spp." *Plant Physiology* 75: 732–739.

Altschul, S. F., W. Gish, W. Miller, E. W. Myers, and D. J. Lipman. 1990. "Basic Local Alignment Search Tool." *Journal of Molecular Biology* 215, no. 3: 403–410. https://doi.org/10.1016/S0022-2836(05)80360-2.

Amaral-Zettler, L. A., E. A. Mccliment, H. W. Ducklow, and S. M. Huse. 2009. "A Method for Studying Protistan Diversity Using Massively Parallel Sequencing of V9 Hypervariable Regions of Small-Subunit

Ribosomal RNA Genes." *PLoS One* 4, no. 7: e6372. https://doi.org/10.1371/journal.pone.0006372.

Anderson, D. M., and D. Wall. 1978. "Potential Importance of Benthic Cysts of *Gonyaulax tamarensis* and *G. excavata* in Initiating Toxic Dinoflagellate Bloom." *Journal of Phycology* 14, no. 2: 224–234. https://doi.org/10.1111/j.1529-8817.1978.tb02452.x.

Anidjar, N., S. N. Giddings, E. Brasseale, A. Rodriguez, and X. Wu. 2024. "Along-channel Exchange Flow Structure in a Seasonally Inverse Low-inflow Estuary." In *Poster Presentation at Physics of Estuaries and Coastal Seas Conference in Bordeaux, France*. https://pecs2024.sciencesconf.org/data/pages/PECS_2024_Book_of_abstracts_1.pdf.

Blake, A. C., D. B. Chadwick, A. Zirino, and I. Rivera-Duarte. 2004. "Spatial and Temporal Variations in Copper Speciation in San Diego Bay." *Estuaries* 27, no. 3: 437–447. https://doi.org/10.1007/BF02803536.

Bokulich, N. A., B. D. Kaehler, J. R. Rideout, et al. 2018. "Optimizing Taxonomic Classification of Marker-Gene Amplicon Sequences With QIIME 2's q2-Feature-Classifier Plugin." *Microbiome* 6, no. 1: 90. https://doi.org/10.1186/s40168-018-0470-z.

Bolyen, E., J. R. Rideout, M. R. Dillon, et al. 2019. "Reproducible, Interactive, Scalable and Extensible Microbiome Data Science Using QIIME 2." *Nature Biotechnology* 37: 852–857.

Bouman, H. A., O. Ulloa, D. J. Scanlan, et al. 2006. "Oceanographic Basis of the Global Surface Distribution of *Prochlorococcus* Ecotypes." *Science* 312, no. 5775: 918–921. https://doi.org/10.1126/science.1122692.

Brahamsha, B. 1996. "A Genetic Manipulation System for Oceanic Cyanobacteria of the Genus *Synechococcus*." *Applied and Environmental Microbiology* 62, no. 5: 1747–1751. https://doi.org/10.1128/AEM.62.5.1747-1751.1996.

Carrigee, L. A., J. P. Frick, J. A. Karty, L. Garczarek, F. Partensky, and W. M. Schluchter. 2021. "MpeV Is a Lyase Isomerase That Ligates a Doubly Linked Phycourobilin on the β-Subunit of Phycoerythrin I and II in Marine *Synechococcus*." *Journal of Biological Chemistry* 296: 100031. https://doi.org/10.1074/JBC.RA120.015289.

Chadwick, D. B., and J. L. Largier. 1999a. "The Influence of Tidal Range on the Exchange Between San Diego Bay and the Ocean." *Journal of Geophysical Research: Oceans* 104, no. C12: 29885–29899. https://doi.org/10.1029/1999jc900166.

Chadwick, D. B., and J. L. Largier. 1999b. "Tidal Exchange at the Bay-Ocean Boundary." *Journal of Geophysical Research: Oceans* 104, no. C12: 29901–29924. https://doi.org/10.1029/1999jc900165.

Chadwick, D. B., J. L. Largier, R. T. Cheng, D. G. Aubrey, C. T. Friedrichs, and Wiley. 1996. "The Role of Thermal Stratification in Tidal Exchange at the Mouth of San Diego Bay." In *Buoyancy Effects on Coastal and Estuarine Dynamics*, edited by D. G. Aubrey and C. T. Friedrichs, 155–174. Washington, DC: Wiley. https://doi.org/10.1029/CE053p0155.

Chen, F., K. Wang, J. Kan, M. T. Suzuki, and K. E. Wommack. 2006. "Diverse and Unique Picocyanobacteria in Chesapeake Bay, Revealed by 16S-23S rRNA Internal Transcribed Spacer Sequences." *Applied and Environmental Microbiology* 72, no. 3: 2239–2243. https://doi.org/10.1128/AEM.72.3.2239-2243.2006.

Chisholm, S. W., R. J. Olson, E. R. Zettler, R. Goericke, J. B. Waterbury, and N. A. Welschmeyer. 1988. "A Novel Free-Living Prochlorophyte Abundant in the Oceanic Euphotic Zone." *Nature* 334, no. 6180: 340–343. https://doi.org/10.1038/334340a0.

Choi, D. H., J. H. Noh, and J.-H. Lee. 2014. "Application of Pyrosequencing Method for Investigating the Diversity of *Synechococcus* Subcluster 5.1 in Open Ocean." *Microbes and Environments* 29, no. 1: 17–22. https://doi.org/10.1264/JSME2.ME13063.

Choi, D. H., J. H. Noh, and J. Shim. 2013. "Seasonal Changes in Picocyanobacterial Diversity as Revealed by Pyrosequencing in Temperate Waters of the East China Sea and the East Sea." *Aquatic Microbial Ecology* 71, no. 1: 75–90. https://doi.org/10.3354/ame01669.

Chrétiennot-Dinet, M.-J., C. Courties, A. Vaquer, et al. 1995. "A New Marine Picoeucaryote: *Ostreococcus tauri* Gen. Et Sp. Nov. (Chlorophyta, Prasinophyceae)." *Phycologia* 34, no. 4: 285–292. https://doi.org/10.2216/i0031-8884-34-4-285.1.

Coale, T., V. Loconte, K. Turk-Kubo, et al. 2024. "Nitrogen-Fixing Organelle in a Marine Alga." *Science* 384: 217–222. https://doi.org/10.1126/science.adk1075.

Collier, J. L., and B. Palenik. 2003. "Phycoerythrin-Containing Picoplankton in the Southern California Bight." *Deep-Sea Research Part II: Topical Studies in Oceanography* 50, no. 14–16: 2405–2422. https://doi.org/10.1016/S0967-0645(03)00127-9.

de la Broise, D., and B. Palenik. 2007. "Immersed In Situ Microcosms: A Tool for the Assessment of Pollution Impact on Phytoplankton." *Journal of Experimental Marine Biology and Ecology* 341, no. 2: 274–281. https://doi.org/10.1016/j.jembe.2006.10.045.

Debelius, B., J. M. Forja, T. A. Delvalls, and L. M. Lubián. 2009. "Toxicity of Copper in Natural Marine Picoplankton Populations." *Ecotoxicology* 18, no. 8: 1095–1103. https://doi.org/10.1007/s10646-009-0377-3.

Debelius, B., J. M. Forja, Á. DelValls, and L. M. Lubián. 2010. "Toxic Effect of Copper on Marine Picophytoplankton Populations Isolated from Different Geographic Locations." *Scientia Marina* 74, no. S1: 133–141. https://doi.org/10.3989/scimar.2010.74s1133.

Doré, H., G. K. Farrant, U. Guyet, et al. 2020. "Evolutionary Mechanisms of Long-Term Genome Diversification Associated With Niche Partitioning in Marine Picocyanobacteria." *Frontiers in Microbiology* 11: 567431. https://doi.org/10.3389/FMICB.2020.567431.

Doré, H., U. Guyet, J. Leconte, et al. 2023. "Differential Global Distribution of Marine Picocyanobacteria Gene Clusters Reveals Distinct Niche-Related Adaptive Strategies." *ISME Journal* 17, no. 5: 720–732. https://doi.org/10.1038/s41396-023-01386-0.

Doré, H., J. Leconte, U. Guyet, et al. 2022. "Global Phylogeography of Marine *Synechococcus* in Coastal Areas Reveals Strong Community Shifts." *MSystems* 7, no. 6: e0065622. https://doi.org/10.1128/msystems.00656-22.

Dufresne, A., M. Ostrowski, D. J. Scanlan, et al. 2008. "Unraveling the Genomic Mosaic of a Ubiquitous Genus of Marine Cyanobacteria." *Genome Biology* 9, no. 5: R90. https://doi.org/10.1186/gb-2008-9-5-r90.

Everroad, R. C., and A. M. Wood. 2012. "Phycoerythrin Evolution and Diversification of Spectral Phenotype in Marine *Synechococcus* and Related Picocyanobacteria." *Molecular Phylogenetics and Evolution* 64, no. 3: 381–392. https://doi.org/10.1016/j.ympev.2012.04.013.

Farrant, G. K., H. Doré, F. M. Cornejo-Castillo, et al. 2016. "Delineating Ecologically Significant Taxonomic Units From Global Patterns of Marine Picocyanobacteria." *Proceedings of the National Academy of Sciences of the United States of America* 113, no. 24: E3365–E3374. https://doi.org/10.1073/pnas.1524865113.

Ferrieux, M., L. Dufour, H. Doré, et al. 2022. "Comparative Thermophysiology of Marine *Synechococcus* CRD1 Strains Isolated From Different Thermal Niches in Iron-Depleted Areas." *Frontiers in Microbiology* 13. https://doi.org/10.3389/fmicb.2022.893413.

Ferris, M. J., and B. Palenik. 1998. "Niche Adaptation in Ocean Cyanobacteria." *Nature* 396, no. 19: 226–228.

Flombaum, P., J. L. Gallegos, R. A. Gordillo, et al. 2013. "Present and Future Global Distributions of the Marine Cyanobacteria *Prochlorococcus* and *Synechococcus*." *Proceedings of the National Academy of Sciences of the United States of America* 110, no. 24: 9824–9829. https://doi.org/10.1073/pnas.1307701110.

Fuller, N. J., D. Marie, F. Partensky, D. Vaulot, A. F. Post, and D. J. Scanlan. 2003. "Clade-Specific 16S Ribosomal DNA Oligonucleotides Reveal the Predominance of a Single Marine *Synechococcus* Clade Throughout a Stratified Water Column in the Red Sea." *Applied and Environmental Microbiology* 69, no. 5: 2430–2443. https://doi.org/10.1128/AEM.69.5.2430-2443.2003.

Gottschalk, S., and M. Kahlert. 2012. "Shifts in Taxonomical and Guild Composition of Littoral Diatom Assemblages Along Environmental Gradients." *Hydrobiologia* 694, no. 1: 41–56. https://doi.org/10.1007/s10750-012-1128-7.

Grébert, T., H. Doré, F. Partensky, et al. 2018. "Light Color Acclimation Is a Key Process in the Global Ocean Distribution of *Synechococcus* Cyanobacteria." *Proceedings of the National Academy of Sciences* 115, no. 9: E2010–E2019. https://doi.org/10.1073/pnas.1717069115.

Guindon, S., J. F. Dufayard, V. Lefort, M. Anisimova, W. Hordijk, and O. Gascuel. 2010. "New Algorithms and Methods to Estimate Maximum-Likelihood Phylogenies: Assessing the Performance of PhyML 3.0." *Systematic Biology* 59, no. 3: 307–321. https://doi.org/10.1093/sysbio/syq010.

Guillard, R. R. L. 1975. "Culture of Phytoplankton for Feeding Marine Invertebrates." In *Culture of Marine Invertebrate Animals*, edited by W. L. Smith and M. H. Chanley, 26–60. Plenum Press.

Hayman, N. T., G. Rosen, M. A. Colvin, et al. 2020. "Seasonal Toxicity Observed With Amphipods (*Eohaustorius estuarius*) at Paleta Creek, San Diego Bay, USA." *Environmental Toxicology and Chemistry* 39, no. 1: 229–239. https://doi.org/10.1002/etc.4619.

Huang, S., S. W. Wilhelm, H. R. Harvey, K. Taylor, N. Jiao, and F. Chen. 2012. "Novel Lineages of *Prochlorococcus* and *Synechococcus* in the Global Oceans." *ISME Journal* 6, no. 2: 285–297. https://doi.org/10.1038/ISMEJ.2011.106.

Hunter-Cevera, K. R., A. F. Post, E. E. Peacock, and H. M. Sosik. 2016. "Diversity of *Synechococcus* at the Martha's Vineyard Coastal Observatory: Insights From Culture Isolations, Clone Libraries, and Flow Cytometry." *Microbial Ecology* 71, no. 2: 276–289. https://doi.org/10.1007/s00248-015-0644-1.

Johnson, Z. I., E. R. Zinser, A. Coe, N. P. McNulty, E. M. S. Woodward, and S. W. Chisholm. 2006. "Niche Partitioning Among *Prochlorococcus* Ecotypes Along Ocean-Scale Environmental Gradients." *Science* 311, no. 5768: 1737–1740. https://doi.org/10.1126/science.1118052.

Katz, C. N. 1998. "Seawater Polynuclear Aromatic Hydrocarbons and Copper in San Diego Bay."

Klempay, B., N. Arandia-Gorostidi, A. E. Dekas, et al. 2021. "Microbial Diversity and Activity in Southern California Salterns and Bitterns: Analogues for Remnant Ocean Worlds." *Environmental Microbiology* 23, no. 7: 3825–3839. https://doi.org/10.1111/1462-2920.15440.

Laber, C. P., B. Pontiller, C. Bunse, et al. 2022. "Seasonal and Spatial Variations in *Synechococcus* Abundance and Diversity Throughout the Gullmar Fjord, Swedish Skagerrak." *Frontiers in Microbiology* 13. https://doi.org/10.3389/fmicb.2022.828459.

Largier, J. 2010. *Low-Inflow Estuaries: Hypersaline, Inverse, and Thermal Scenarios*. Cambridge University Press. https://doi.org/10.1017/CBO9780511676567.010.

Largier, J. L. 2023. "Recognizing Low-Inflow Estuaries as a Common Estuary Paradigm." *Estuaries and Coasts* 46: 1949–1970. https://doi.org/10.1007/s12237-023-01271-1.

Largier, J. L., C. J. Hearn, and D. B. Chadwick. 1996. "Density Structures in Low Inflow Estuaries." In *Buoyancy Effects on Coastal and Estuarine Dynamics*, edited by D. G. Aubrey and C. T. Friedrichs, 227–241. American Geophysical Union.

Largier, J. L., J. T. Hollibaugh, and S. V. Smith. 1997. "Seasonally Hypersaline Estuaries in Mediterranean-Climate Regions." *Estuarine, Coastal and Shelf Science* 45, no. 6: 789–797. https://doi.org/10.1006/ecss.1997.0279.

Larkin, A. A., and A. C. Martiny. 2017. "Microdiversity Shapes the Traits, Niche Space, and Biogeography of Microbial Taxa." *Environmental Microbiology Reports* 9, no. 2: 55–70. https://doi.org/10.1111/1758-2229.12523.

Larkin, A. A., A. R. Moreno, A. J. Fagan, A. Fowlds, A. Ruiz, and A. C. Martiny. 2020. "Persistent El Niño Driven Shifts in Marine Cyanobacteria Populations." *PLoS One* 15 (9): e0238405. https://doi.org/10.1371/journal.pone.0238405.

Le Jeune, A. H., M. Charpin, V. Deluchat, et al. 2006. "Effect of Copper Sulphate Treatment on Natural Phytoplanktonic Communities." *Aquatic Toxicology* 80, no. 3: 267–280. https://doi.org/10.1016/j.aquatox.2006.09.004.

Lê, S., J. Josse, and F. Husson. 2008. "FactoMineR: An R Package for Multivariate Analysis." *Journal of Statistical Software* 25, no. 1: 1–18. https://doi.org/10.18637/jss.v025.i01.

Lee, M. D., N. A. Ahlgren, J. D. Kling, et al. 2019. "Marine *Synechococcus* Isolates Representing Globally Abundant Genomic Lineages Demonstrate a Unique Evolutionary Path of Genome Reduction Without a Decrease in GC Content." *Environmental Microbiology* 21, no. 5: 1677–1686. https://doi.org/10.1111/1462-2920.14552.

Letunic, I., and P. Bork. 2021. "Interactive Tree of Life (iTOL) v5: An Online Tool for Phylogenetic Tree Display and Annotation." *Nucleic Acids Research* 49, no. W1: W293–W296. https://doi.org/10.1093/nar/gkab301.

Li, G., Q. Song, P. Zheng, et al. 2021. "Dynamics and Distribution of Marine *Synechococcus* Abundance and Genotypes During Seasonal Hypoxia in a Coastal Marine Ranch." *Journal of Marine Science and Engineering* 9, no. 5. https://doi.org/10.3390/jmse9050549.

Li, S., Y. Dong, X. Sun, et al. 2024. "Seasonal and Spatial Variations of *Synechococcus* in Abundance, Pigment Types, and Genetic Diversity in a Temperate Semi-Enclosed Bay." *Frontiers in Microbiology* 14. https://doi.org/10.3389/fmicb.2023.1322548.

Lucas, A. J., C. L. Dupont, V. Tai, J. L. Largier, B. Palenik, and P. J. S. Franks. 2011. "The Green Ribbon: Multiscale Physical Control of Phytoplankton Productivity and Community Structure Over a Narrow Continental Shelf." *Limnology and Oceanography* 56, no. 2: 611–626. https://doi.org/10.4319/lo.2011.56.2.0611.

Mahmoud, R. M., J. E. Sanfilippo, A. A. Nguyen, et al. 2017. "Adaptation to Blue Light in Marine *Synechococcus* Requires MpeU, an Enzyme With Similarity to Phycoerythrobilin Lyase Isomerases." *Frontiers in Microbiology* 8. https://doi.org/10.3389/fmicb.2017.00243.

Malmstrom, R. R., A. Coe, G. C. Kettler, et al. 2010. "Temporal Dynamics of *Prochlorococcus* Ecotypes in the Atlantic and Pacific Oceans." *ISME Journal* 4, no. 10: 1252–1264. https://doi.org/10.1038/ismej.2010.60.

Martin, M. 2011. "Cutadapt Removes Adapter Sequences From High-Throughput Sequencing Reads." *EMBnet. Journal* 17, no. 1: 10–12. https://doi.org/10.14806/ej.17.1.200.

Mascarenhas, V., and T. Keck. 2018. "Marine Optics and Ocean Color Remote Sensing." In *YOUMARES 8 – Oceans Across Boundaries: Learning From Each Other*, 41–54. Cham: Springer International Publishing. https://doi.org/10.1007/978-3-319-93284-2_4.

Mazard, S., M. Ostrowski, F. Partensky, and D. J. Scanlan. 2012. "Multi-Locus Sequence Analysis, Taxonomic Resolution and Biogeography of Marine *Synechococcus*." *Environmental Microbiology* 14, no. 2: 372–386. https://doi.org/10.1111/j.1462-2920.2011.02514.x.

Mcdonald, D., M. N. Price, J. Goodrich, et al. 2012. "An Improved Greengenes Taxonomy With Explicit Ranks for Ecological and Evolutionary Analyses of Bacteria and Archaea." *ISME Journal* 6: 610–618. https://doi.org/10.1038/ismej.2011.139.

Moore, L. R., M. Ostrowski, D. J. Scanlan, K. Feren, and T. Sweetsir. 2005. "Ecotypic Variation in Phosphorus-Acquisition Mechanisms Within Marine Picocyanobacteria." *Aquatic Microbial Ecology* 39, no. 3: 257–269. https://doi.org/10.3354/ame039257.

Moore, L. R., A. F. Post, G. Rocap, and S. W. Chisholm. 2002. "Utilization of Different Nitrogen Sources by the Marine Cyanobacteria *Prochlorococcus* and *Synechococcus*." *Limnology and Oceanography* 47, no. 4: 989–996. https://doi.org/10.4319/lo.2002.47.4.0989.

Mühling, M., N. J. Fuller, A. Millard, et al. 2005. "Genetic Diversity of Marine *Synechococcus* and Co-Occurring Cyanophage Communities: Evidence for Viral Control of Phytoplankton." *Environmental Microbiology* 7, no. 4: 499–508. https://doi.org/10.1111/j.1462-2920.2005.00713.x.

Nagarkar, M., M. Wang, B. Valencia, and B. Palenik. 2021. "Spatial and Temporal Variations in *Synechococcus* Microdiversity in the Southern California Coastal Ecosystem." *Environmental Microbiology* 23, no. 1: 252–266. https://doi.org/10.1111/1462-2920.15307.

Neira, C., L. A. Levin, G. Mendoza, and A. Zirino. 2014. "Alteration of Benthic Communities Associated With Copper Contamination Linked to Boat Moorings." *Marine Ecology* 35, no. 1: 46–66. https://doi.org/10.1111/maec.12054.

Novick, A., and L. Szilard. 1950. "Experiments With the Chemostat on Spontaneous Mutation of Bacteria." *PNAS* 36: 708–719. https://www.pnas.org.

Ong, L. J., A. N. Glazer, and J. B. Waterbury. 1984. "An Unusual Phycoerythrin From a Marine Cyanobacterium." *Science* 224, no. 4644: 80–83. https://doi.org/10.1126/science.224.4644.80.

Palenik, B. 1994. "Cyanobacterial Community Structure as Seen From RNA Polymerase Gene Sequence Analysis." *Applied and Environmental Microbiology* 60, no. 9: 3212–3219.

Palenik, B. 2001. "Chromatic Adaptation in Marine *Synechococcus* Strains." *Applied and Environmental Microbiology* 67, no. 2: 991–994. https://doi.org/10.1128/AEM.67.2.991-994.2001/ASSET/9D04E35C-363D-4A0D-A6EF-E6923FE35403/ASSETS/GRAPHIC/AM0211549003.JPEG.

Parada, A. E., D. M. Needham, and J. A. Fuhrman. 2016. "Every Base Matters: Assessing Small Subunit rRNA Primers for Marine Microbiomes With Mock Communities, Time Series and Global Field Samples." *Environmental Microbiology* 18, no. 5: 1403–1414. https://doi.org/10.1111/1462-2920.13023.

Paytan, A., K. R. M. Mackey, Y. Chen, et al. 2009. "Toxicity of Atmospheric Aerosols on Marine Phytoplankton." *PNAS* 106: 4601–4605.

Paz-Yepes, J., B. Brahamsha, and B. Palenik. 2013. "Role of a Microcin-C-Like Biosynthetic Gene Cluster in Allelopathic Interactions in Marine *Synechococcus*." *Proceedings of the National Academy of Sciences of the United States of America* 110, no. 29: 12030–12035. https://doi.org/10.1073/pnas.1306260110.

Pittera, J., F. Humily, M. Thorel, D. Grulois, L. Garczarek, and C. Six. 2014. "Connecting Thermal Physiology and Latitudinal Niche Partitioning in Marine *Synechococcus*." *ISME Journal* 8, no. 6: 1221–1236. https://doi.org/10.1038/ismej.2013.228.

Rammel, T., M. Nagarkar, and B. Palenik. 2024. "Temporal and Spatial Diversity and Abundance of Cryptophytes in San Diego Coastal Waters." *Journal of Phycology* 60: 668–684. https://doi.org/10.1111/jpy.13451.

Rocap, G., D. L. Distel, J. B. Waterbury, and S. W. Chisholm. 2002. "Resolution of *Prochlorococcus* and *Synechococcus* Ecotypes by Using 16S-23S Ribosomal DNA Internal Transcribed Spacer Sequences." *Applied and Environmental Microbiology* 68, no. 3: 1180–1191. https://doi.org/10.1128/AEM.68.3.1180-1191.2002.

Rodriguez, A. R. 2019. *Buoyancy Transport Mechanisms at Continental Shelf, Surf Zone, and Estuarine Scales*. PhD. Thesis. La Jolla, CA: UC San Diego.

Sanfilippo, J. E., L. Garczarek, F. Partensky, and D. M. Kehoe. 2019. "Chromatic Acclimation in Cyanobacteria: A Diverse and Widespread Process for Optimizing Photosynthesis." *Annual Review of Microbiology* 73: 407–433. https://doi.org/10.1146/annurev-micro-020518.

Scanlan, D. J., M. Ostrowski, S. Mazard, et al. 2009. "Ecological Genomics of Marine Picocyanobacteria." *Microbiology and Molecular Biology Reviews* 73, no. 2: 249–299. https://doi.org/10.1128/mmbr.00035-08.

Six, C., J.-C. Thomas, L. Garczarek, et al. 2007. "Diversity and Evolution of Phycobilisomes in Marine *Synechococcus* Spp.: A Comparative Genomics Study." *Genome Biology* 8, no. 12: 259. https://doi.org/10.1186/gb-2007-8-12-r259.

Sohm, J. A., N. A. Ahlgren, Z. J. Thomson, et al. 2016. "Co-Occurring *Synechococcus* Ecotypes Occupy Four Major Oceanic Regimes Defined by Temperature, Macronutrients and Iron." *ISME Journal* 10, no. 2: 333–345. https://doi.org/10.1038/ISMEJ.2015.115.

Sorensen, K., B. Swope, and V. Kirtay. 2013. "Marine Ecologic Index Survey of San Diego Bay."

Stoeck, T., D. Bass, M. Nebel, et al. 2010. "Multiple Marker Parallel Tag Environmental DNA Sequencing Reveals a Highly Complex Eukaryotic Community in Marine Anoxic Water." *Molecular Ecology* 19: 21–31. https://doi.org/10.1111/j.1365-294X.2009.04480.x.

Stuart, R. K., B. Brahamsha, K. Busby, and B. Palenik. 2013. "Genomic Island Genes in a Coastal Marine *Synechococcus* Strain Confer Enhanced Tolerance to Copper and Oxidative Stress." *ISME Journal* 7, no. 6: 1139–1149. https://doi.org/10.1038/ismej.2012.175.

Stuart, R. K., C. L. Dupont, D. A. Johnson, I. T. Paulsen, and B. Palenik. 2009. "Coastal Strains of Marine *Synechococcus* Species Exhibit Increased Tolerance to Copper Shock and a Distinctive Transcriptional Response Relative to Those of Open-Ocean Strains." *Applied and Environmental Microbiology* 75, no. 15: 5047–5057. https://doi.org/10.1128/AEM.00271-09.

Tai, V., R. S. Burton, and B. Palenik. 2011. "Temporal and Spatial Distributions of Marine *Synechococcus* in the Southern California Bight Assessed by Hybridization to Bead-Arrays." *Marine Ecology Progress Series* 426: 133–147. https://doi.org/10.3354/meps09030.

Tai, V., and B. Palenik. 2009. "Temporal Variation of *Synechococcus* Clades at a Coastal Pacific Ocean Monitoring Site." *ISME Journal* 3, no. 8: 903–915. https://doi.org/10.1038/ismej.2009.35.

Toledo, G., and B. Palenik. 1997. "*Synechococcus* Diversity in the California Current as Seen by RNA Polymerase (rpoC1) Gene Sequences of Isolated Strains." *Applied and Environmental Microbiology* 63, Issue 11: 4298–4303.

Toledo, G., and B. Palenik. 2003. "A *Synechococcus* Serotype Is Found Preferentially in Surface Marine Waters." *Limnology and Oceanography* 48, no. 5: 1744–1755. https://doi.org/10.4319/lo.2003.48.5.1744.

Toledo, G., B. Palenik, and B. Brahamsha. 1999. "Swimming Marine *Synechococcus* Strains With Widely Different Photosynthetic Pigment Ratios Form a Monophyletic Group." *Applied and Environmental Microbiology* 65, no. 12: 5247–5251.

Wang, T., X. Chen, J. Li, and S. Qin. 2022. "Phylogenetic Structure of Synechococcus Sssemblages and Its Environmental Determinants in the Bay and Strait Areas of a Continental Sea." *Frontiers in Microbiology* 13. https://doi.org/10.3389/fmicb.2022.757896.

Wang, T., X. Xia, J. Chen, H. Liu, and H. Jing. 2022. "Spatio-Temporal Variation of *Synechococcus* Assemblages at DNA and cDNA Levels in the Tropical Estuarine and Coastal Waters." *Frontiers in Microbiology* 13. https://doi.org/10.3389/fmicb.2022.837037.

Wickham, H. 2016. "ggplot2: Elegant Graphics for Data Analysis." Springer-Verlag . https://ggplot2.tidyverse.org.

Wood, M. A., D. A. Phinney, and C. S. Yentsch. 1998. "Water Column Transparency and the Distribution of Spectrally Distinct Forms of Phycoerythrin-Containing Organisms." *Marine Ecology Progress Series* 162: 25–31.

Xia, X., S. Cheung, H. Endo, K. Suzuki, and H. Liu. 2019. "Latitudinal and Vertical Variation of *Synechococcus* Assemblage Composition Along 170° W Transect From the South Pacific to the Arctic Ocean." *Microbial Ecology* 77, no. 2: 333–342. https://doi.org/10.1007/s00248-018-1308-8.

Xia, X., F. Partensky, L. Garczarek, et al. 2017. "Phylogeography and Pigment Type Diversity of *Synechococcus* Cyanobacteria in Surface

Waters of the Northwestern Pacific Ocean." *Environmental Microbiology* 19, no. 1: 142–158. https://doi.org/10.1111/1462-2920.13541.

Xia, X., N. K. Vidyarathna, B. Palenik, P. Lee, and H. Liu. 2015. "Comparison of the Seasonal Variations of *Synechococcus* Assemblage Structures in Estuarine Waters and Coastal Waters of Hong Kong." *Applied and Environmental Microbiology* 81, no. 21: 7644–7655. https://doi.org/10.1128/AEM.01895-15.

Yilmaz, P., L. W. Parfrey, P. Yarza, et al. 2014. "The SILVA and "All-Species Living Tree Project (LTP)" taxonomic Frameworks." *Nucleic Acids Research* 42, no. D1: D643–D648. https://doi.org/10.1093/nar/gkt1209.

Zhou, B., J. Ma, F. Chen, et al. 2020. "Mechanisms Underlying Silicon-Dependent Metal Tolerance in the Marine Diatom *Phaeodactylum tricornutum*." *Environmental Pollution* 262: 114331. https://doi.org/10.1016/j.envpol.2020.114331.

Zwirglmaier, K., L. Jardillier, M. Ostrowski, et al. 2008. "Global Phylogeography of Marine *Synechococcus* and *Prochlorococcus* Reveals a Distinct Partitioning of Lineages Among Oceanic Biomes." *Environmental Microbiology* 10, no. 1: 147–161. https://doi.org/10.1111/j.1462-2920.2007.01440.x.

Supporting Information

Additional supporting information can be found online in the Supporting Information section.